

Copyright  
by  
Ryan C. Fulcher  
2016

**The Thesis Committee for Ryan C. Fulcher  
Certifies that this is the approved version of the following thesis:**

**Temperature Fluctuation Analysis for GRACE Twin Satellites**

**APPROVED BY  
SUPERVISING COMMITTEE:**

**Supervisor:**

---

Ofodike A. Ezekoye

---

Srinivas Bettadpur

---

John R. Howell

# **Temperature Fluctuation Analysis for GRACE Twin Satellites**

**by**

**Ryan C. Fulcher, B.S.M.E.**

**Thesis**

Presented to the Faculty of the Graduate School of

The University of Texas at Austin

in Partial Fulfillment

of the Requirements

for the Degree of

**Master of Science in Engineering**

**The University of Texas at Austin**

**August 2016**

## **Acknowledgements**

I would like to thank Dr. John Howell and Dr. Srinivas Bettadpur for allowing me to join this project, and for their involvement with the effort. I would also like to thank Dr. Ofodike Ezekoye for joining my thesis committee, and acting as my co-supervisor.

This material is based upon work supported by the National Aeronautics and Space Administration (NASA) under Contract No. NNL14AA00C.

## **Abstract**

### **Temperature Fluctuation Analysis for GRACE Twin Satellites**

Ryan C. Fulcher, M.S.E.

The University of Texas at Austin, 2016

Supervisor: Ofodike A. Ezekoye

The overall objective of this research project is to find patterns and give a rudimentary explanation of these patterns in how heat flows through and around the GRACE Twin Satellites. Specifically, investigation of an unexplained frequency found in the temperature fluctuations gives rise to a new understanding of heat transfer in a complex mechanical system found in a near-vacuum environment. Impartial and unhindered information for this experiment come from two primary sources: the first is archived thermal analyses performed by the original manufacturers prior to the satellites' launch in March 2002, and the second is current data feeds constantly streaming from the active satellites in orbit. The relevant data being extracted from this library of information for the purposes of this investigation are recorded at various time intervals, and taken from many locations, which are all discussed. These variables are used to run new simulations in attempt to recreate the original thermal analysis. Finally, significant changes in temperature leads to small thermal expansions, which can add noise to other data gathered by the satellites.

## Table of Contents

List of Figures .....	viii
<b>PART 1: <i>SURVEY OF THE SATELLITE SYSTEM</i> .....</b>	<b>1</b>
<b>Chapter 1: Introduction and Methodology .....</b>	<b>2</b>
<b>Chapter 2: The Comprehensive Thermal Environment .....</b>	<b>7</b>
<b>MODES OF HEAT TRANSFER .....</b>	<b>7</b>
<b>BETA PRIME ANGLE .....</b>	<b>8</b>
<b>UMBRA AND PENUMBRA .....</b>	<b>8</b>
<b>SOLAR FLUX .....</b>	<b>10</b>
<b>ALBEDO FACTOR .....</b>	<b>10</b>
<b>EARTH INFRARED .....</b>	<b>11</b>
<b>SATELLITE INTERIOR .....</b>	<b>12</b>
<b>Chapter 3: Overview of Temperature Fluctuations .....</b>	<b>18</b>
<b>HEATER EFFECTS .....</b>	<b>18</b>
<b>BETA PRIME AND ECCENTRICITY .....</b>	<b>21</b>
<b>FREQUENCY INVESTIGATION .....</b>	<b>26</b>
<b>PART 2: <i>SENSITIVITY ANALYSIS</i> .....</b>	<b>31</b>
<b>Chapter 4: The Numerical Model Inputs .....</b>	<b>32</b>
<b>SOLAR RADIATION .....</b>	<b>32</b>
<b>ALBEDO FACTOR .....</b>	<b>36</b>
<b>EARTH INFRARED RADIATION .....</b>	<b>36</b>
<b>RESISTANCE HEATERS AND ELECTRIC CURRENT .....</b>	<b>37</b>
<b>Chapter 5: Results from Numerical Analyses .....</b>	<b>39</b>
<b>ENERGY BALANCE FOR TEMPERATURE ESTIMATION .....</b>	<b>39</b>
<b>MODEL OUTPUTS .....</b>	<b>44</b>

<b>Chapter 6: Conclusions and Suggestions .....</b>	<b>47</b>
Glossary .....	52
References .....	54

## List of Figures

Figure 1:	Temperature plot for PCDU and Magnetometer .....	5
Figure 2:	Beta Prime plotted with Shadow Time .....	9
Figure 3:	Internal View of GRACE Satellite .....	13
Figure 4:	Total Power Consumption with a 16 cycle/day filter .....	14
Figure 5:	Battery Voltage FFT: Low beta prime angle .....	16
Figure 6:	Battery Voltage FFT: High beta prime angle .....	17
Figure 7:	Mode $C_{20}$ of Geopotential over GRACE Mission .....	19
Figure 8:	Mode $C_{21}$ of Geopotential over GRACE Mission .....	19
Figure 9:	Average temperature of several components for a decade .....	20
Figure 10:	Beta Prime Angle over life of GRACE Mission.....	23
Figure 11:	Temperature of OBDH plotted with Shadow Time for 2009 .....	24
Figure 12:	Temperature of OBDH plotted with Shadow Time for 2007 .....	25
Figure 13:	Temperature Plot of OBDH .....	27
Figure 14:	Spectral Analysis of OBDH.....	28
Figure 15:	Spectral Analysis of RFEA Heater and Temperature .....	29
Figure 16:	Spectral Analysis of PCDU Heater and Temperature.....	29
Figure 17:	Region of Umbra and Penumbra.....	34
Figure 18:	Change of Solar Irradiance .....	35
Figure 19:	Temperature of Energy Balance vs. Telemetry .....	42
Figure 20:	FFT of Energy Balance vs. Telemetry .....	43
Figure 21:	OBDH Telemetry vs. Simulation Temperature: Natural Heat Only.	44
Figure 22:	OBDH Telemetry vs. Simulation Temperature: Natural Heat and Heaters .....	45



Figure 23:	OBDH Telemetry vs. Simulation Temperature: All Heat Inputs .....	46
Figure 24:	FFT Plot of Total Incoming Solar Power .....	48
Figure 25:	FFT Plot of Transmitter Power .....	50

## **PART 1: *SURVEY OF THE SATELLITE SYSTEM***

The following three chapters will examine what is physically occurring in the open system of the two satellites. The characterization of temperature fluctuations, transfer of heat by radiation and conduction, and various electrical systems will all be considered. Real-time telemetry files that are regularly transferred directly from the satellites' on-board computer systems will provide all the necessary information needed in Part 1. The intention of this section will be to completely describe the satellite system and surroundings from all perspectives, and to lay down context for the reasoning process of conclusions that may arise thereafter.

## **Chapter 1: Introduction and Methodology**

The primary mission of the GRACE Twin Satellites, launched in March of 2002, is to bring new understanding to the time-variable gravitational field of the Earth. Other methods have been used to attempt this using numerous other satellites already in orbit, but the GRACE Satellites are the first to employ the use of two satellites with the sole purpose of measuring the gravity field using their relative motion. As such, greater details have now been made available to researchers. Exploration of the gravity field can lead to a number of results, since this field is a function of mass distribution. Primarily, it brings a new perspective to earth science fields such as hydrology, geodesy, or oceanography; but more broadly speaking, information can be gleaned on the changing climate over the lifetime of the mission.

Using GPS tracking and microwave emitters on board these satellites, the distance between their respective centers of mass can easily be calculated. As the front satellite approaches an abnormality in the gravity field, the force from the gravity pulls on the satellite, briefly causing the velocity to increase. The front satellite then moves past the said gravity irregularity. Moments later, the second satellite collides with the same gravity field anomaly and produces similar results for that point in space. Over the duration of several days, the satellites traverse the entire surface of the earth. This information is relayed back to researchers, giving them data to “map” the gravity field. The microwave K-band ranging instrument, which tracks these variations, are sensitive and can detect particularly small changes in distance. Unfortunately, however, small thermal expansions and contractions can lead to noise in the data. This is caused by the changing position of

the satellites relative to the sun, their primary heat source, as well as the eclipsing factor of the earth in the satellites' path. Heat is also generated internally to keep the satellite temperatures within a specified threshold. It would be likely for the oscillation of generated heat to match the orbital frequency, since the control systems for the heaters are temperature dependent, but the power output of each component will be considered individually.

By analyzing temperature data from the satellite, an unaccountable pattern in the frequency of temperature change has been revealed. It is expected for the temperature to adjust with the satellite motion, and have the same frequency as the orbit. However, a secondary periodicity of two cycles per day was consistently found in the temperatures of all internal components. For future researchers to be able to accurately predict how the thermal expansions might change the gravity data streaming from the satellites, it is important to have a complete understanding of temperature fluctuations and their causes. The aim of this paper is to thoroughly scrutinize the temperature oscillation abnormality by first taking every possible source of heat- both external and internal- into account, and various explanations for the irregularity will then be proposed in light of these heat inputs. The relevant fluctuation patterns were systematically explored using several investigation methods. With a new understanding of the thermal patterns and use of updated software that was not available to the original manufacturers, guidelines can now be produced for future analyses.

The first step of the process used here was an investigation of the actual temperatures taken at several different time intervals, and at various points across the

satellite. Several thermistors are placed at key points throughout each satellite, and they automatically record temperatures roughly every minute. From a spatial perspective, specific thermistors were chosen for the analysis to highlight their proximity to heaters or other components, or what degree of insulation from the outside environment is present. Meanwhile, to further investigate the transient character, various time scales were studied that ranged from a few hours to the entire GRACE mission to get a clearer picture of the difference between local and global variables. For instance, certain satellite components with sensitive equipment had to have a highly controlled temperature, while other components protruded outside the spacecraft, and were completely exposed to the space environment. Consequently, the latter case was much more affected by the external heat sources. Naturally, this was apparent when viewing the temperature data. To illustrate this, Figure 1 is a plot of two temperature variation cases occurring during an arbitrary five-day period. The blue curve belongs to the Power Conditioning and Distribution Unit (PCDU), and has a range of approximately  $2.1\text{ }^{\circ}\text{C}$ , while the red curve, belonging to the Magnetometer, varies about  $25.5\text{ }^{\circ}\text{C}$ . The PCDU can be found near the center of the satellite, whereas the Magnetometer is inside the protruding S-Band Boom antenna, and is thus more susceptible to temperature change due to solar flux and earth infrared radiation. Any equipment that is even more subject to error or damage from the changing temperature would have near-constant temperature plots that result from a highly controlled thermal environment.

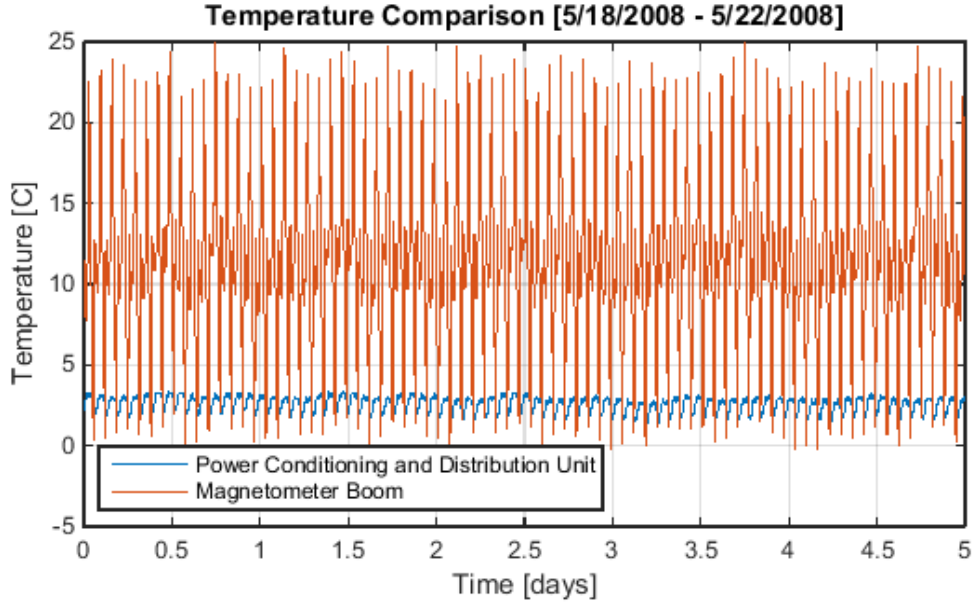


Figure 1: Temperature plot for PCDU and Magnetometer

Internally, the power output  $P$  of the heaters also needed to be calculated. Given documented load resistances  $R$ , and voltage readings  $v$  from the library of satellite telemetry data, the Equation 1 is used:

$$P_{heater} = \delta \frac{v^2}{R} \quad (1)$$

The third necessary variable for this equation,  $\delta$ , is a Boolean value that is also recorded by the satellite. It is set to one when the heater is turned on, and zero otherwise. The satellites report the values for both the voltage and the Boolean every three seconds.

The final consideration was of various electrical components that are not necessarily tasked with heating the satellite, but produce heat nonetheless by simply having an electric current. These components do not have their resistances listed in the literature from the satellite design specifications, but in this case, current readings  $I$  can be extracted directly. The power is then calculated by the following equation:

$$P_i = Iv \quad (2)$$

where  $i$  is the component number. Note that the Boolean variable  $\delta$  is missing from Equation 2 since the current inherently takes this on and off nature into account. Due to the principle of Conservation of Energy, electrical power must be converted to either heat or motion. Since the amount of energy spent on moving parts is negligible on this particular spacecraft, it is assumed all electrical energy is dissipated as waste heat.

The second part of this experiment, an account that begins in Chapter 4, was to solve a fundamental energy balance equation of the whole satellite thermal system for an average temperature, while simultaneously using the Finite Element Method to find the temperatures of individual components of the satellite. These results are then compared to telemetry temperatures- which are first summarized in Chapter 3. Parameters include the set of heat sources from the electrical components, radiation from the sun and the earth, and heat transfer (conduction and radiation) between each component within the satellite, as well as the physical geometry of the spacecraft. These parameters are outlined in the following chapter.

## **Chapter 2: The Comprehensive Thermal Environment**

The GRACE Twin Satellites began their mission at an altitude of 500 kilometers with an  $89^\circ$  inclination, and now cruise at an altitude closer to 360 kilometers. They take approximately ninety minutes to complete one cycle around the earth. During this journey, several variables must be taken into account to accurately predict the temperature scale of the satellite as a whole, as well as all the individual components. The system will not be treated as steady state, since the satellite stores energy, and heat is not immediately reradiated back to space precisely when it enters the spacecraft. Additionally, the orientation of the satellite orbit plane, defined by the beta prime angle, will cycle throughout the year, which then directly impacts the environment surrounding the satellites. This has an immediate effect on how much heat flows from the sun and the earth in the form of radiation. Further, the changing surface of the earth directly below the travelling satellites will consequently have a varying infrared radiation output and magnitude of reflected sunlight. The decrease in altitude does not lead to a significant difference in solar radiation, due to the proportionately much larger distance between the earth and the sun. However, it can affect how much infrared radiation from the earth is received.

### **MODES OF HEAT TRANSFER**

Prior to describing each of the possible heat sources, it is important to first note there are no external fluids, due to the vacuum of the space environment. Indeed, there are no fluids at all except for the thruster fuel, throughout the entire satellite system, and therefore little convective heat transfer takes place. All heat transfer that will be discussed has been brought about entirely by way of radiation, whether that be from the sun, the earth,



or even between the internal components; or by conduction via physical contact within the satellite.

### **BETA PRIME ANGLE**

The first and possibly most important variable considered is the beta prime angle, defined as the angle between the plane of satellite orbital motion and the vector pointing from the earth to the sun. The effect of this angle can be subcategorized into two major cases: perpendicular and parallel. The first has a beta prime angle of  $\pm 90^\circ$ , where positive is defined such that the satellite is moving counter-clockwise when viewed as an observer on the sun. In this circumstance, the satellite never crosses into the shadow of the earth, and makes contact with a relatively constant inflow of solar radiation. The opposite extreme would place the plane of rotation of the orbit parallel to the earth-sun vector, or in other words, the beta prime angle is zero. In this case then, the satellites spend the largest fraction of time per orbit in the shadow of the earth, which can be up to approximately 36 minutes.

The beta prime angle takes roughly 325 days for one complete cycle. In one day, this angle will change 0.3%. Thus, if it is desired to study the temperatures for a relatively short period of time, such as a few days, this angle can be treated as a constant. However, the changing angle must be taken into account when considering longer periods of time. When considering multiple years, for instance, data was collected at the same point in the beta prime cycle, rather than the same day of the calendar cycle.

### **UMBRA AND PENUMBRA**

When the beta prime angle is greater than roughly  $\pm 68^\circ$ , the satellites spend no time in the shadow of the earth. As the angle decreases from this critical value, this period slowly increases to a maximum of about 36 minutes per orbit, as mentioned before, which

occurs at a beta prime angle of 0. When travelling along their orbit, the twin satellites encounter two somewhat distinct shadow regions. The first region the satellites briefly experience is named penumbra, where the earth only partially obscures the incoming sunlight. The satellites then travel out of the ambiguous section of penumbra into umbra. In this sector, the solar radiation is completely blocked. The following plot, whose data was taken from the year 2008, demonstrates a correlation between the changing beta prime angle, and how much time per orbit the satellites spend eclipsed by the earth, shown as Figure 2. It must be noted, however, that although the satellites may spend more time per orbit in the earth shadow when the beta prime angle is low, the surface area that is exposed to the direct solar rays is larger. In contrast, when the beta prime angle is high, the exposed surface of each satellite is the side, which has smaller dimensions. Thus, a lower magnitude of solar energy may be absorbed, despite the satellites never entering the region of umbra.

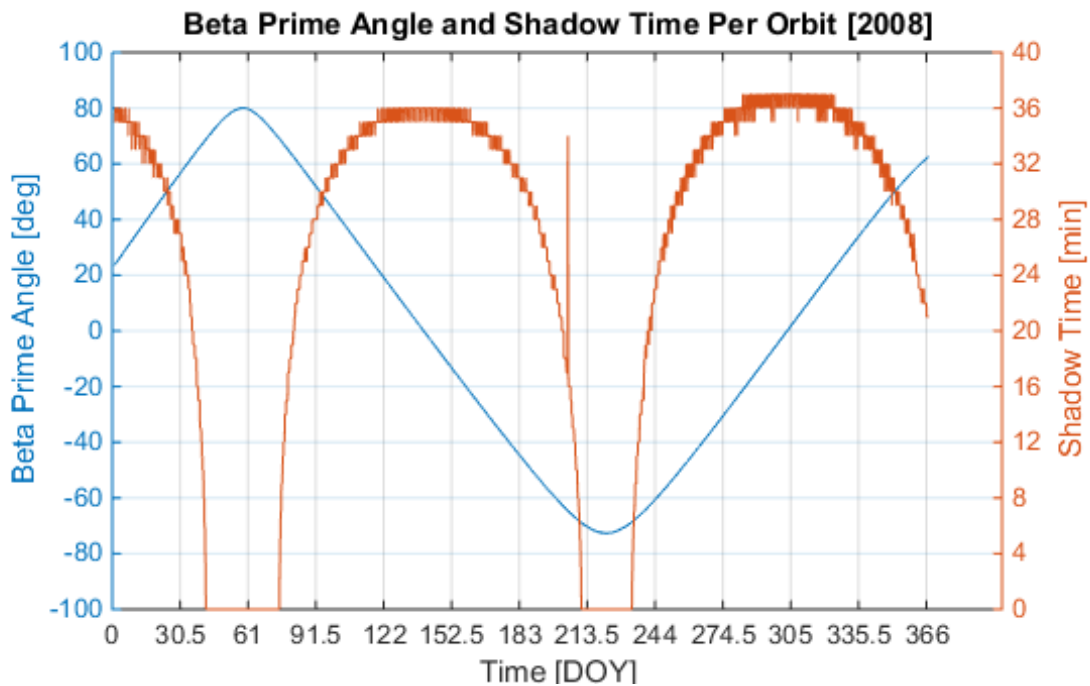


Figure 2: Beta Prime plotted with Shadow Time

## **SOLAR FLUX**

Aside from the earth periodically eclipsing the satellites, a comprehensive investigation of the value of the solar flux itself would reveal that it is not, in fact, a constant. Due to the eccentricity of the earth's orbit, the distance from the sun to the earth can change about 3% within a year [2-3], and consequently so does the solar flux. Nevertheless, the average value of  $1367.5 \text{ W/m}^2$  from an annual perspective is typically considered adequate when generating initial design specifications for spacecraft [2]. This has remained relatively unchanged in the lifetime of the GRACE mission [1]. However, in an attempt to fully understand the nature of the heat flow through the satellite, the changing solar flux within a year must be taken into account. When the earth is closest to the sun, which occurs in early January, the solar flux has a value of  $1414 \text{ W/m}^2$ , and conversely in early July, when the earth is furthest from the sun, the solar flux is around  $1323 \text{ W/m}^2$  [2-3]. How this affects the GRACE Satellites will be explored in a later chapter, but since the change spans a year, a value can be calculated and averaged as a constant for relatively short periods of time.

Additionally to the steady change of the solar flux constant, the incoming sun rays are approximately straight relative to the earth-sun vector, due to such a large distance from this source- about 149.6 million kilometers. Simultaneously, the satellite is itself in constant motion. Consequently, the exterior of the satellite is receiving the solar radiation at a continuously changing angle. This angle, and the resulting view factor, will then have a dramatic effect on which components of each satellite collects more heat.

## **ALBEDO FACTOR**

Not only do the satellites receive light directly from the sun, but a portion of this radiation is reflected off the surface of the earth. Thus, the earth albedo needs to be taken into account. The rotation of the earth, weather patterns, and the satellite motion all can

change what surface lies below the satellites at any given moment. Surfaces like fresh snow will reflect as much as 70% of the incoming solar flux back to the satellite, whereas a dense forest will reflect as little as 10% [4, 9]. Simultaneous to the changing satellite position, the weather patterns affect cloud cover. Clouds will reflect anywhere from 10% to 90% depending on humidity, or air water density, back to the bottom surface of the spacecraft [4, 10]. Subsequently, although there are methods to predicting the exact albedo factor, it has proven to be difficult and beyond the scope of this research project. Future research will benefit from further exploration of how to accurately predict the exact albedo factor at any given position of the spacecraft. Nevertheless, aside from these uncertainties, it is clear that the albedo factor is only relevant when the satellite is not in the shadow of the earth. Thus, the timing of the albedo factor is the same as that of the solar flux, regardless of its magnitude. For this project, an average constant value of 30% was used [2, 6, 8].

## **EARTH INFRARED**

The earth additionally emits its own radiation at the infrared frequency, and it also varies with location on the surface of the earth and weather patterns. When albedo is high, such as at the polar regions of the earth, this infrared radiation decreases. The maximum would be found around the earth equator in the tropical regions. As with the albedo factor, cloud cover will also tend to have an effect on the amount of earth radiation received, though the effect is opposite, as the clouds in this case act as a thermal blanket, reducing the amount of radiation that reaches the spacecraft. Lastly, as mentioned before, the altitude can also have more of an effect on the changing infrared radiation than the changing solar flux, since the source is much closer. In summary, the total average ranges from approximately  $227 \text{ W/m}^2$  to  $251 \text{ W/m}^2$  [2]. Nevertheless, as with the solar flux

constant, an average value of  $234 \text{ W/m}^2$  is typically used for initial design specifications [2]. For the purposes of this project, this average was used.

### **SATELLITE INTERIOR**

To more accurately determine various causes for temperature fluctuations, a brief inventory of a satellite must be taken. As mentioned before, certain components may be found in an environment where the temperatures are highly regulated. In contrast, other components protrude off the exterior of the satellite, and are much more susceptible to external thermal inputs. Figure 3 is a sketch of the layout of the satellite system. It must be noted that the positive X-axis is defined as pointing toward the other satellite, rather than in the direction of forward momentum. This decision was made to simplify calculations. The Z-axis always points in the Nadir direction (toward the Earth), and the Y-axis points according to the right-hand rule convention. The set of axes for this orientation is included in Figure 3.

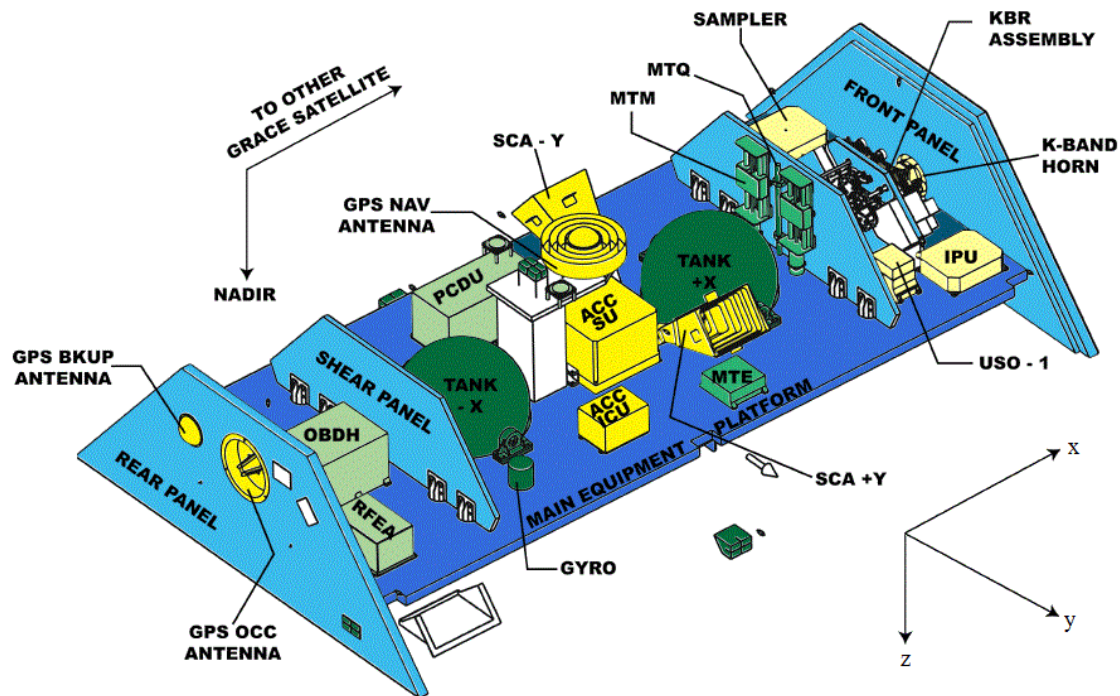


Figure 3: Internal View of GRACE Satellite

The top and side surfaces of each satellite are covered in a solar array of silicon cells- not shown in the figure above. Some energy is dissipated to the environment, but most is transferred to on-board batteries. The batteries then provide energy for the rest of the spacecraft. The heaters operate using high resistances, but other components generate some heat by simply having an electric current. This heat dissipation will be investigated more thoroughly later in this chapter. Again not shown, the bottom exterior is a radiator, rather than another solar panel. The radiator provides the greatest means of total heat dissipation, due to its particularly large area, surface properties, and its orientation relative to the earth. Because of this, the satellites have no need for an active cooling system.

Each of the two satellites carry a total of 64 resistance heaters, spaced intermittently throughout the spacecraft, depending on how thermally sensitive a component may be. Heaters can also be found in the protruding instruments such as the S-band boom, so that

the thermal behaviors of these external elements are not completely regulated by the space environment. Since there is very little convection, these heaters provide heat entirely by conduction and radiation.

It was previously noted that all electrical components generate heat due to power dissipation. Figure 4 is a plot of the total power consumption of all the electrical components, which was calculated using Equation 2 shown in Chapter 1. The effects from the orbital motion are distinct, and can even overshadow a possible secondary frequency. Thus, to further understand the pattern of change in the power consumption, a filter has been added to exclude the 16 cycle per day oscillation pattern, emphasizing the secondary frequency.

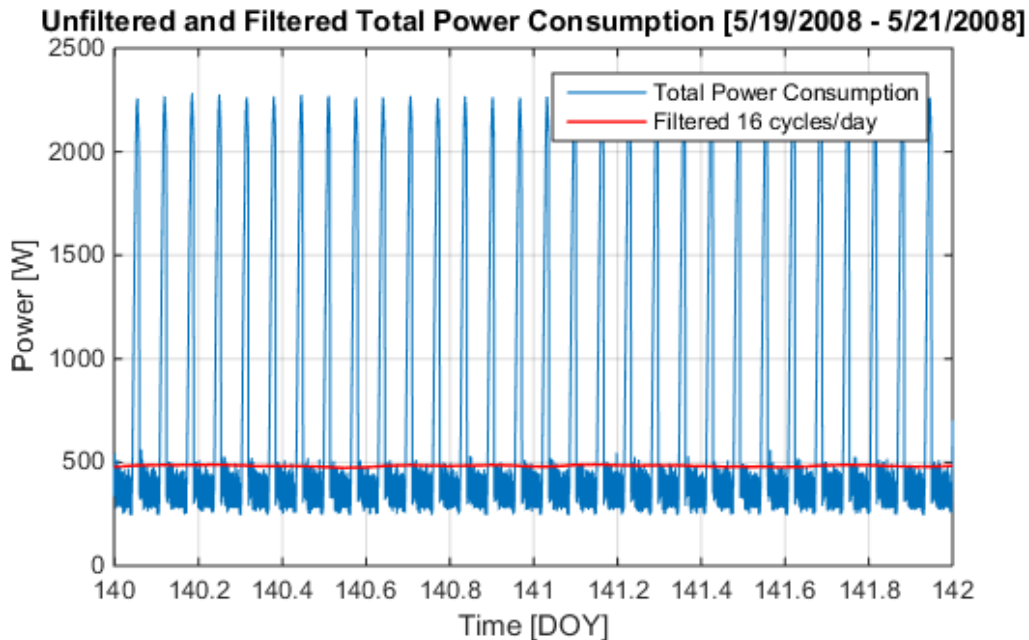


Figure 4: Total Power Consumption with a 16 cycle/day filter

When trying to better understand the behavior of the temperature fluctuations, these underlying frequencies in related variables all need to be thoroughly explored. This

process can trace the main cause of the twice per day frequency found in the resulting temperature plots. From the plot above, a pattern that matches the temperatures has now been revealed in the total electrical power consumption. The next step will be to consider each of the electrical systems individually in order to pinpoint the source of the behavior of the temperature variability. Since the heaters are directly correlated with the temperatures, they were the first to be analyzed.

To save power in more recent years, the satellites entered into “thermal survival mode” at the end of 2008, and the heaters were given a lower threshold temperature than what was originally programmed in the early mission. The result is that there are now periods of time when the heaters do not activate at all. It is during these times that it can be more easily determined if the heaters are either causing the temperatures to oscillate two times per day, or instead a temperature controller is leading the heaters to fluctuate at this rate. Since the heaters do have similar frequencies to the temperatures, it may be thought that the temperatures are directly caused by the heater output. Additionally, if this pattern ceases in the thermistor readings during the phase of the mission when the heaters were deactivated, the source of this secondary oscillation rate has been found. Otherwise, if the temperature abnormality continues after survival mode began, it can be concluded that the temperature change is actually causing the heater power output frequency, and something else is driving the twice per day recurrence. In this case, each of the remaining electrical elements will have to be considered, as their activation is not temperature-dependent.

Excluding heaters, a total of sixteen electrical components per satellite were each comprehensively investigated. The solar panels converted the incoming sunlight to usable energy which was then stored in the batteries. Since there was only one voltage variable throughout the whole spacecraft, this was first investigated by itself by way of a Fast Fourier Transform (FFT) frequency versus amplitude plot for various time periods. These



time periods were chosen at different beta prime angles and different distances from the sun, though it was found the latter made little difference. The next plot, Figure 5, show a voltage FFT plot when the beta prime angle is minimized. The data provided for this particular plot had been taken after survival mode had been initiated, so heaters were active, but minimally.

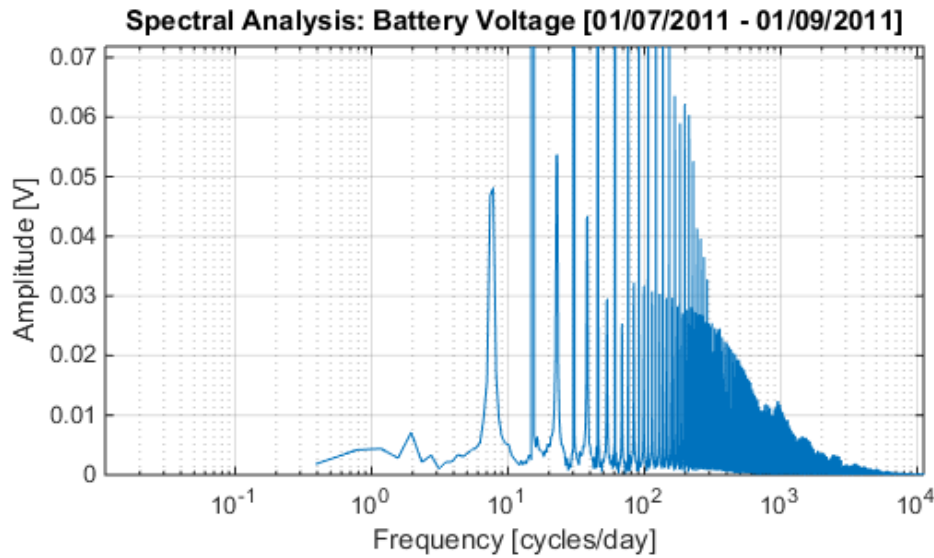


Figure 5: Battery Voltage FFT: Low beta prime angle

The frequency of two cycles per day is evident, but harmonics are seen at multiples of 16 cycles per day due to shadowing of the earth. The following plot, Figure 6, has voltage data taken from the same year, but the beta prime angle in this plot is maximized, so that the earth shadow is not a factor. The changing view factor is now the sole driver for any oscillations found at 16 cycles per day, and the amplitude for this frequency has been diminished. More importantly, however, is that there was no power consumed by the heaters during this time period.

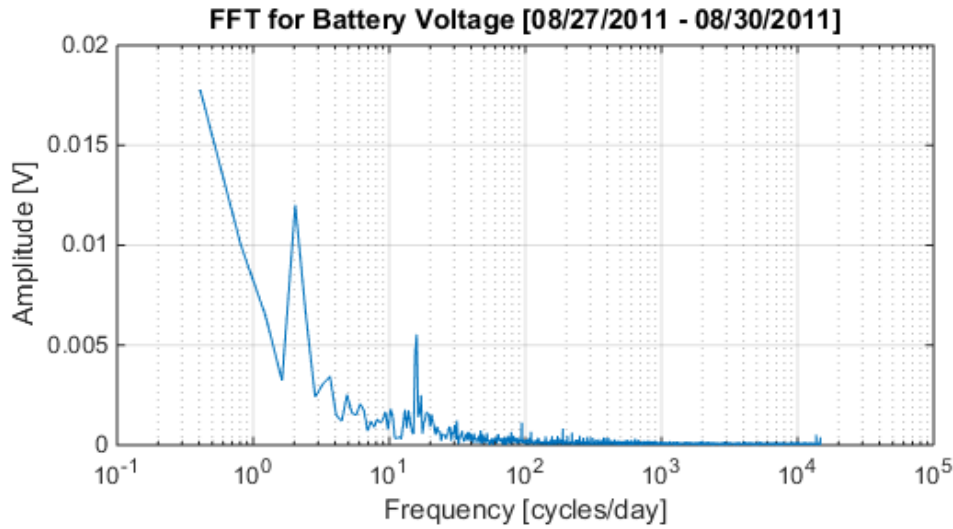


Figure 6: Battery Voltage FFT: High beta prime angle

Two cycles per day is a frequency that is consistently found in the voltage of the collective electrical components, even after the satellites entered survival mode. This secondary frequency seems to be independent of the beta prime angle, as well as the temperature change, since the remaining electrical components are not coupled to the thermistors. The following chapter will more rigorously cover the entire temperature behavior of the satellite system.

### **Chapter 3: Overview of Temperature Fluctuations**

As mentioned in Chapter 1, the patterns found in the physical temperature readings must be viewed from multiple perspectives to gain a clearer understanding of the overall satellite system. Thus, different time spans, different types of analyses, and different locations within the system all contribute a unique view of the heat movement. Variability may be studied at the same location in the two separate satellites. However, it is more important to study two points on two extremes of one satellite, such as the leading edge compared to the trailing edge, or internal compared to external. The reasoning behind this is that the temperature change of a location within one spacecraft will reflect the thermal behavior of its immediate surroundings, whereas the thermal behavior of two identical spacecrafts will be symmetric. Time scales range from a few individual orbits to the entirety of the GRACE mission. Short term variability is useful for understanding aliasing of any one month, while long term is useful studying the mission timescale. When searching for any unaccountable patterns present in the extracted data, they would reveal themselves under extensive examination.

#### **HEATER EFFECTS**

When considering the entire lifespan of the satellite mission, the conditions from year to year were relatively unchanged until the year 2008. However, beginning in the year 2008, the satellite had begun thermal survival mode. To further demonstrate this, Figure 7 and Figure 8 represent two images that plot the behavior of the error in the selected degree-2 harmonics of the earth's potential. This error is defined as the GRACE estimates of the gravitational harmonics minus an empirical quadratic, plus a period fit representation of

the signal. The increased scatter of points in the later years is indicative of potential thermal influences on the geopotential, as the thermal environment on the science instruments was, at this time, successfully less-controlled [15].

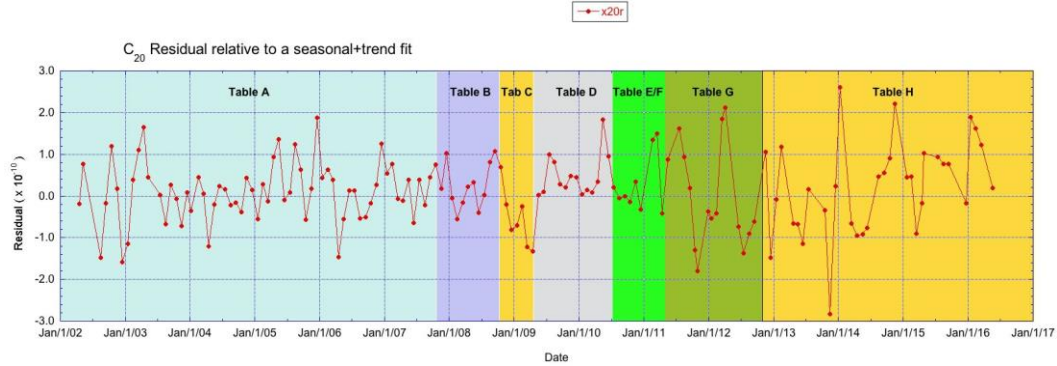


Figure 7: Mode  $C_{20}$  of Geopotential over GRACE Mission

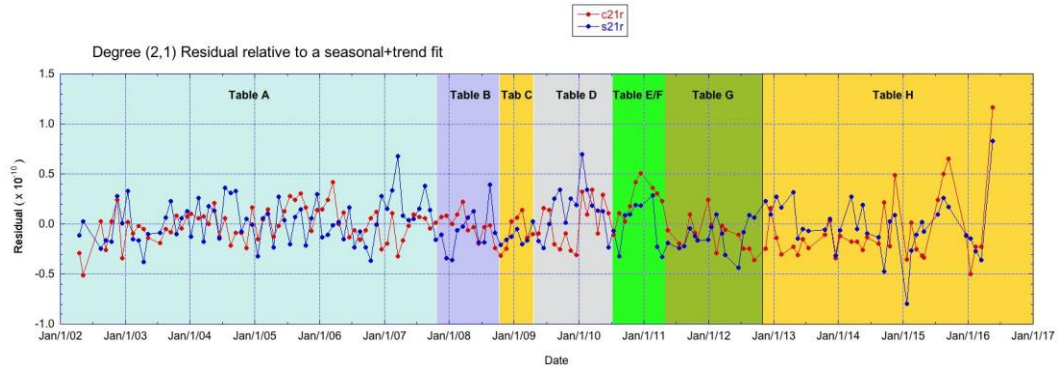


Figure 8: Mode  $C_{21}$  of Geopotential over GRACE Mission

As briefly stated before, this is a mechanism for the satellite to save power by only expending energy where absolutely necessary. In 2010, the satellites decreased the power output to the heaters again. Thus for instance, if the heater output from 2008 were to be compared to that of 2014, much more energy was spent in the earlier time frame. In other words, it is important to take into account for future calculations that much less heat is generated internally by the heaters, even though other electrical systems remained active

and did not decrease in power. Therefore, a relatively steady average temperature is expected from the initial launch date to 2008, and then a slight decline due to power saving mechanisms in the on-board heaters, and a further reduction in 2010 due to a drop in allowable power use. Figure 9 is a plot of the average temperature of several components, taken for the time span of a decade. The reduction of heater output is clearly evident.

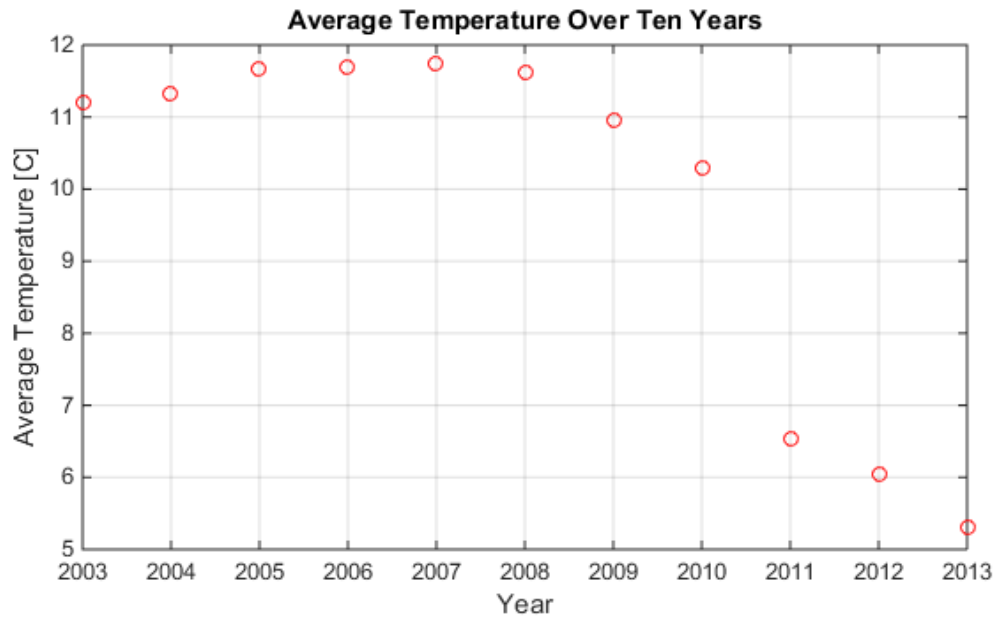


Figure 9: Average temperature of several components for a decade

How this long-term heater power decrease has an effect on short-term temperature fluctuations will be examined further at the end of this chapter. Analyzing the temperature oscillation rate before and after this decrease in heater power will provide some insight as to whether the heaters contribute to the previously noted two cycle per day frequency. This will be investigated more carefully in a later section using another FFT plot.

## BETA PRIME AND ECCENTRICITY

For a given year, there are two main external factors that are guiding the temperature fluctuations: The beta prime angle of the satellite orbit, and the eccentricity of the earth's orbit. Due to the eccentricity, the annual average of the solar flux constant that the earth receives does not change significantly, but it does in fact vary within a year with the distance from the earth to the sun [11]. The eccentricity, whose value is currently about 0.0167, does fluctuate, but only over the span of approximately 100,000 years [3]. This translates to a change in the distance from the earth to the sun of about five million kilometers- which is only 3% of the average orbit radius of 149 million kilometers. We receive a proportional change in the solar flux constant. At Perihelion, the closest the earth comes to the sun, the value of solar flux constant is  $1414 \text{ W/m}^2$ , and conversely at Aphelion when the earth is at its furthest point from the sun, the value is  $1323 \text{ W/m}^2$  [2, 11]. These two events occur in early January and early July, respectively. It must be noted that we do not notice this difference on the surface of the earth, nor does it have a significant effect on the changing seasons. Nevertheless, when analyzing minute changes in the satellites' temperatures and rates of heat transfer throughout each spacecraft, this must take this into account.

The beta prime angle is defined as the angle between the plane on which the satellite orbits and the vector stretching from the center of the earth to the center of the sun, with  $0^\circ$  being when the plane is parallel to the sun vector. This angle is a much more significant condition to be considered when analyzing the temperatures for any given year, as the amount of solar irradiance received by the spacecraft exterior is directly proportional to this angle. From approximately  $\pm 68^\circ$  to  $\pm 90^\circ$ , the satellites transition into a relatively short, three week period where they do not cross into the shadow of the earth at all and receive a steady inflow of solar radiation. Simultaneously, from the perspective of the sun,

the satellite is on its side. The surface being viewed is angled and is not normal to the incoming sun rays. Therefore, despite the constant inflow of solar radiation, the satellite may not absorb all of the heat, and temperatures may actually decrease, depending on the view factor from the sun to the satellite surface.

The extreme opposite occurs when the beta prime angle nears  $0^\circ$  and the plane of rotation is roughly parallel to the vector stretching from the earth to the sun. During this phase, the time spent in the earth's shadow is maximized around 36 minutes per orbit. However, now the head, zenith, and tail of the satellites more often make direct contact with the incoming solar radiation, and are all roughly normal to these sun rays. Hence, even though a large amount of time per orbit is spent in the shadow of the Earth, the satellites are still able to absorb a high volume of solar radiation. The following equation relates the actual solar energy absorbed by the spacecraft to the angle of the normal of the surface, as well as the solar irradiance and surface absorptivity:

$$q_{actual} = q_{sol}\alpha \cos(\theta) \quad (3)$$

$q_{sol}$  is the solar irradiance, or solar flux constant as defined previously,  $\alpha$  is the absorptivity of the satellite exterior, and  $\theta$  is the angle between the light rays and the surface normal.

Figure 11 and Figure 12 show the correlation between the temperatures and the shadow time for the On Board Data Handling (OBDH) system for 2007 and 2009. It must be pointed out that this system is found at the front end of the first satellite, or the back end of the second satellite. In contrast, the temperature plot for a component resting in the middle of the satellite- the Power Control and Distribution Unit (PCDU) for instance- will also reflect the shadow time, but it follows the actual beta prime plot much more closely, rather than the shadow time plot, even though these two variables are inseparable. Finally,

for an external protrusion such as the Magnetometer, the view factor dependence is negligible and the temperatures simply rise when the beta prime angle is high and the shadow time nears zero. Therefore, regardless of the component location, the beta prime angle is always the guiding factor in temperature fluctuations (except obviously in the case of a highly thermally regulated component, where the heaters kept the temperature roughly constant until the year 2008).

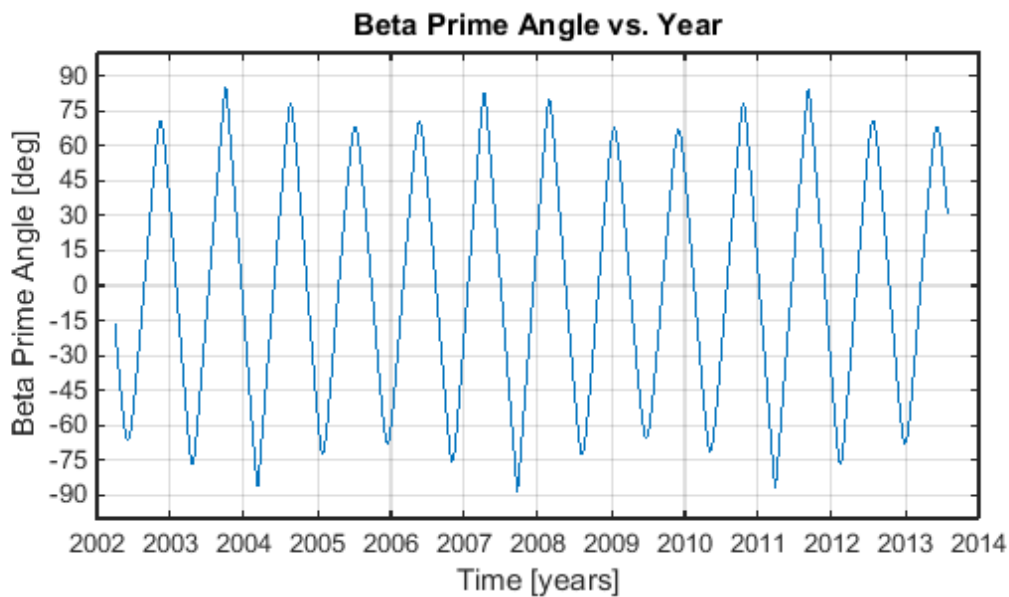


Figure 10: Beta Prime Angle over life of GRACE Mission

Figure 10 represents how the beta prime angle has changed over the lifetime of the GRACE Satellites' mission. The smaller frequency is about one cycle every 325 days, and the larger frequency is one cycle approximately every three and a half years. Because of the resonance in these two cycles, there are occasional years where the absolute value of the angle never exceeds  $68^\circ$ , and thus the satellites never have an orbit without shadow time. It would be during these years that the view factor is never minimized, so for some components- particularly the OBDH in the leading satellite- temperatures will remain



higher than usual. Nevertheless, the lack of heater output that year still brought about an overall average temperature drop in 2009, as shown in Figure 9. Figure 11 shows the direct relationship between the time span in shadow, which as stated before depends on the beta prime angle, plotted against the temperature of the OBDH system for 2009. Figure 12 is a similar plot, but instead from 2007 to emphasize the correlation between time in shadow (and thus the beta prime angle) and temperature. During this particular year, the beta prime angle reaches a value of  $88^\circ$  - far exceeding the threshold value of  $68^\circ$ . Note the sudden temperature minimums when the satellite spends no time in the earth shadow, caused by the low view factor.

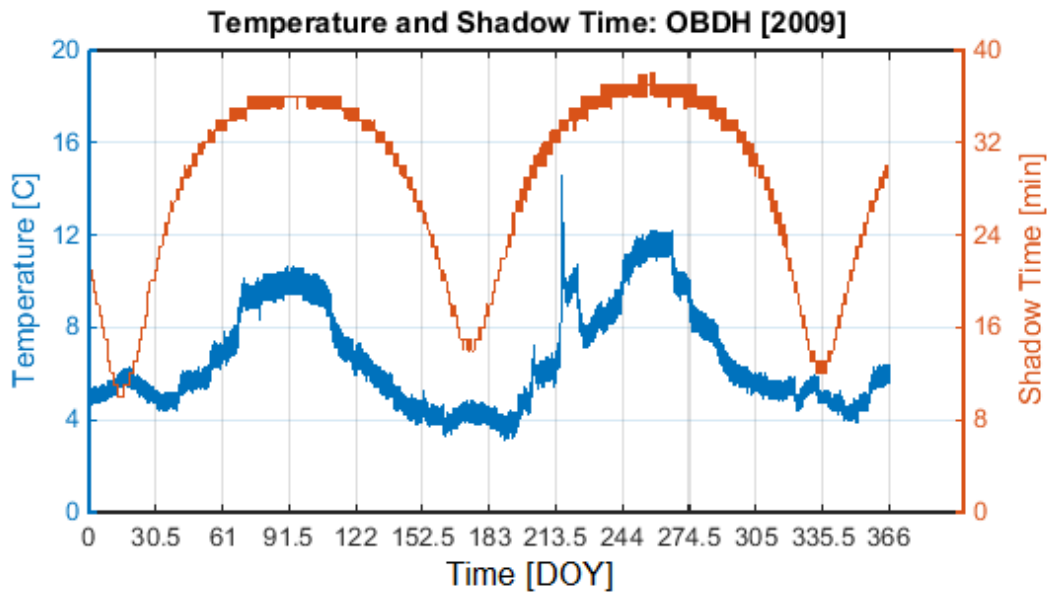


Figure 11: Temperature of OBDH plotted with Shadow Time for 2009

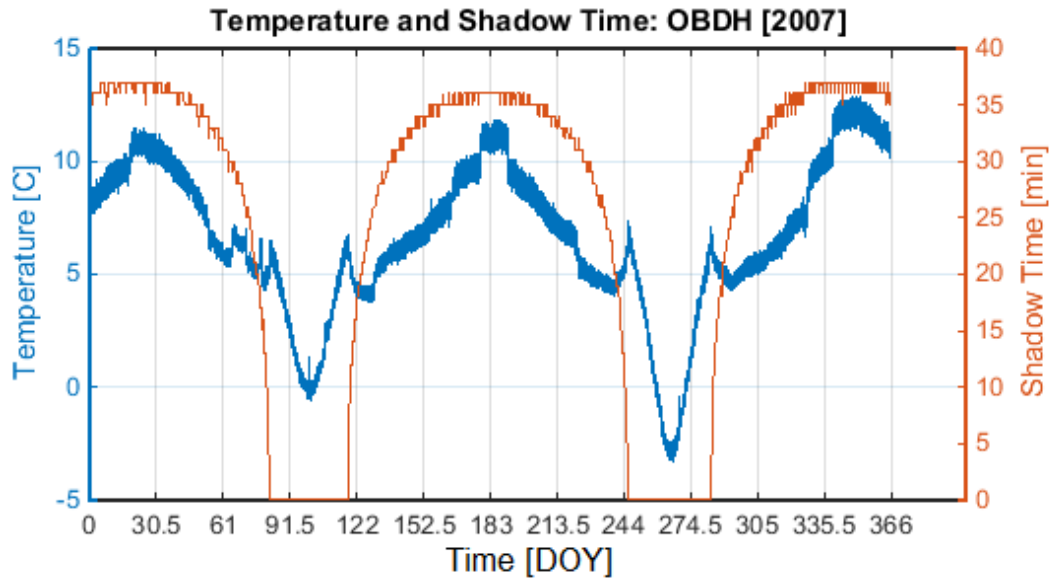


Figure 12: Temperature of OBDH plotted with Shadow Time for 2007

From this investigation, it is made apparent how much of an effect the beta prime angle can have on the thermal environment of the spacecraft. The satellites do briefly experience an increase in temperature when they enter the period of time where they are not eclipsed by the earth, as the view factor of the solar panel on one side is maximized. These side panels have the largest surface area, except for the radiator, and thus can absorb more heat as long as the sun vector is perpendicular to their surface. They are positioned, however, at an angle of  $50^\circ$  from the spacecraft's radiator. Therefore, when the beta prime angle is  $\pm 90^\circ$ , this slope of the solar panel is now  $130^\circ$  from the earth-sun vector, which reduces the solar radiation input by approximately 35%, using Equation 3. From Figure 12, the temperature immediately reduces as the beta prime angle is maximized, or when the time per orbit the satellites are in the earth shadow is zero.

## **FREQUENCY INVESTIGATION**

A Fast Fourier Transform (FFT) spectral analysis is a very useful method for determining the dominant frequencies found in the temperature fluctuations. However, care must be taken to choose the most effective time series. If a time span is chosen that is too long, the beta prime angle may change too much. As a result, the amplitude of the oscillations may begin to change as well, which will distort the results. In contrast, if the time span of the data set is too small, separating the twice per day modulation of 16 cycles per day from the 16 cycle per day variations will be impossible. Thus, it was found that the ideal time span must be longer than one day, but must not exceed ten days. Therefore, the most common time span analyzed was one week long as shown in the plot below, though occasionally this varied by a day or two. One main advantage to viewing data that only extends a week was that frequencies were often revealed that could easily be verified visually. The next two figures show this analysis for the OBDH for two separate weeks: One in February, and one in May. The first is simply a set of temperatures extracted from the satellites over the given week.

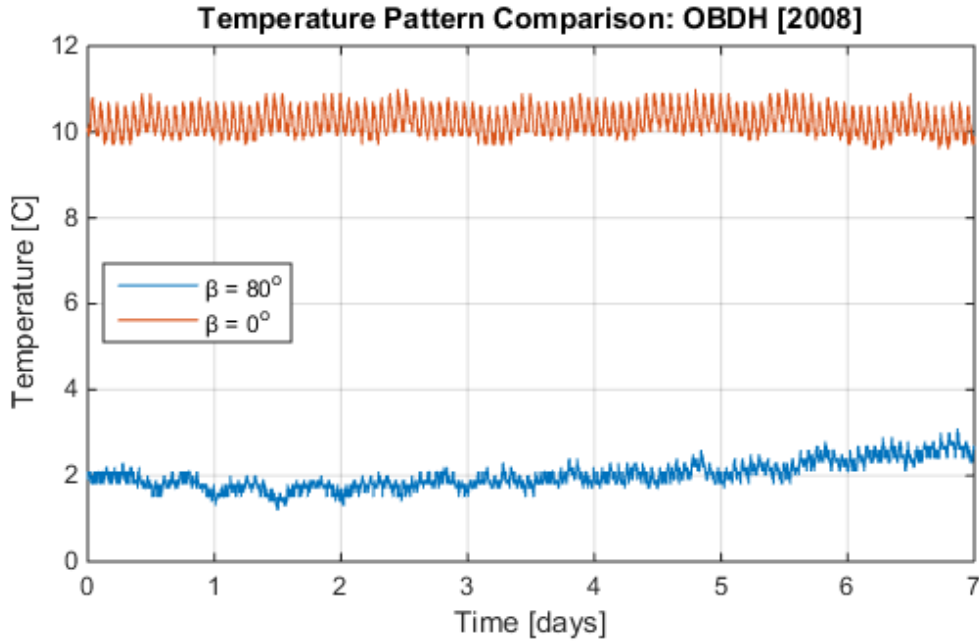


Figure 13: Temperature Plot of OBDH

These two sets of data were chosen to emphasize the effects of two extremes of the beta prime angle. As previously shown in Figures 11 and 12, the mean temperature is much greater when the beta prime angle is minimized. Aside from the difference in the temperature mean value, however, the primary focus of Figure 13 is to demonstrate the amplitude difference of the temperature oscillations at the 16 cycle per day frequency of these two weeks, while the amplitude of the twice per day frequency is approximately equal. In 2008, the beta prime angle is maximized at a value of approximately  $80^\circ$  in February, and it is minimized to zero in May. From this plot, we can see that at the 16 cycle per day frequency, the temperatures fluctuate much less when the satellites receive a more steady inflow of solar radiation, and thus a smaller amplitude in the oscillations. In contrast, when the satellites pass in and out of the earth shadow repeatedly- when the beta prime angle is near  $0^\circ$  as in May of 2008- the temperature variability is much greater. Despite this, it can now be assumed that the twice per day oscillation is not greatly affected

by the changing beta prime angle. This information is confirmed with the following FFT plot for the same time spans. The sharpest rise in amplitude occurs at sixteen cycles per day in the May time series, and is much greater at this frequency than in the February time series. However, the two cycle per day frequency is much more similar in both time frames. Note the plot's x-axis has a logarithmic scale.

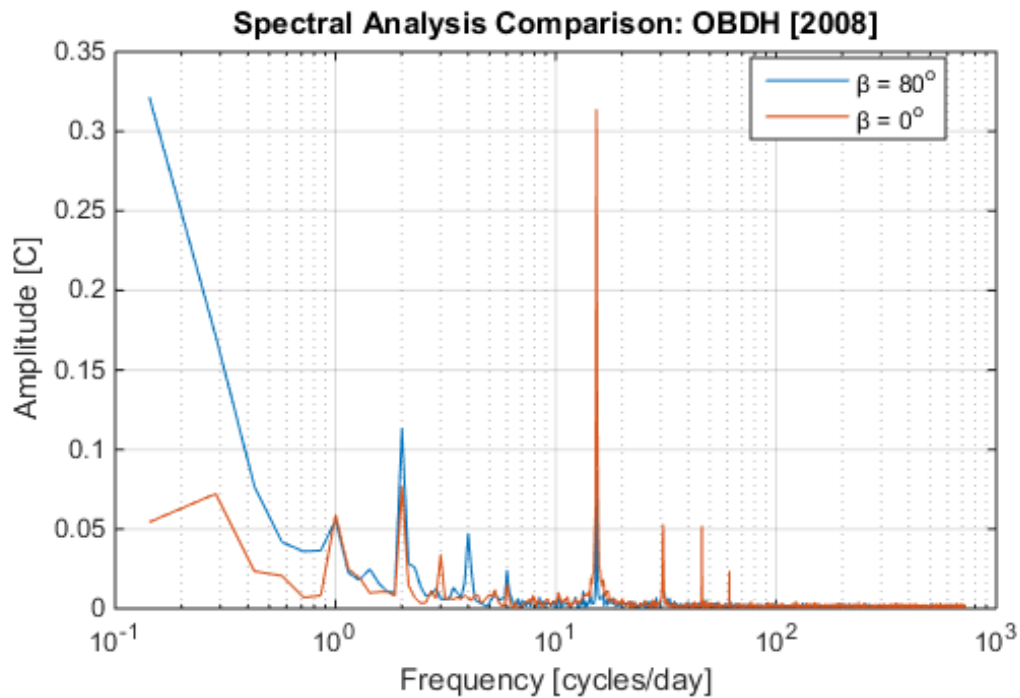


Figure 14: Spectral Analysis of OBDH

An oscillation at two cycles per day is consistent in any time series throughout the year, though the temperatures of some components may fluctuate at a different amplitude, depending on their locations. A similar plot can be produced for the heaters before the satellites entered survival mode, but an FFT analysis does not always return a dominant frequency at two cycles per day. This oddity is shown in Figures 15 and 16.

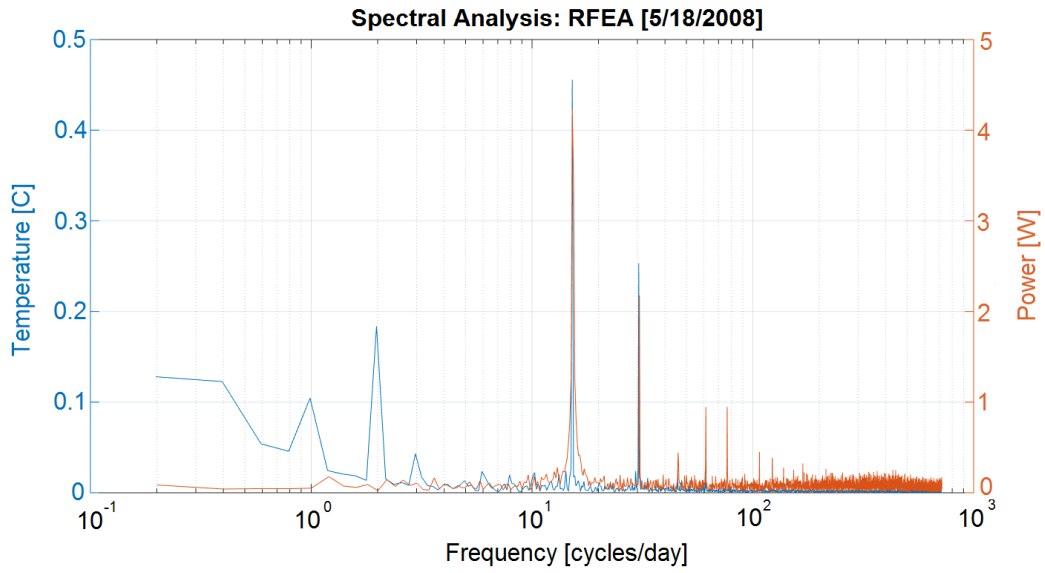


Figure 15: Spectral Analysis of RFEA Heater and Temperature

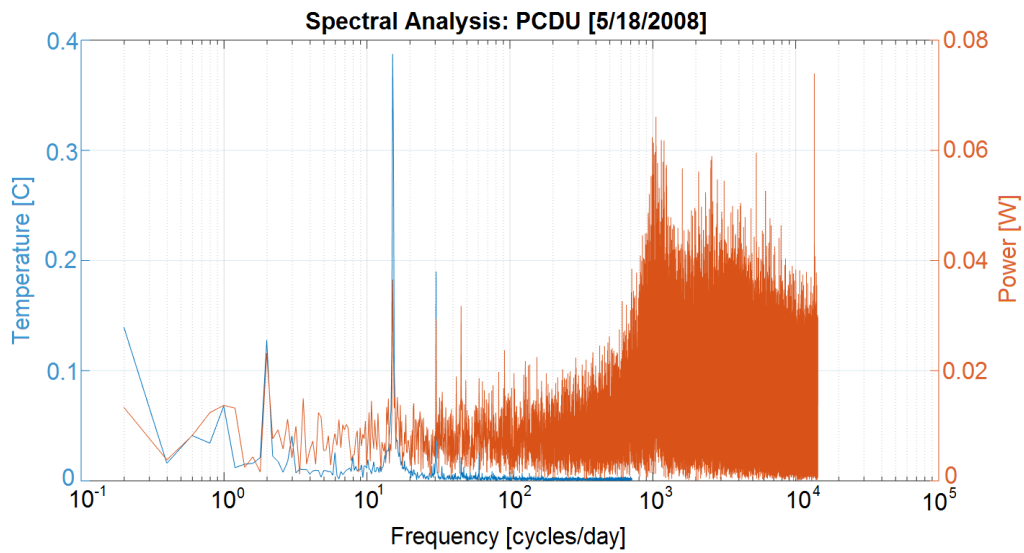


Figure 16: Spectral Analysis of PCDU Heater and Temperature

Ignoring the noise at higher frequencies, the heater for RFEA has no frequency at two cycles per day, whereas the heater for PCDU does. Additionally, the temperature

variability continues to have a dominant frequency at two cycles per day even after 2010 when the satellites drastically reduced the heater power output. Therefore, this solidifies the idea that the heaters do not cause the temperatures to fluctuate at this rate, and any frequency in the heater data at this value are more likely caused by the changing temperature. Consequently, other techniques will need to be employed to understand the source of this lower frequency, such as a computational method. All known parameters will be taken into account in attempt to replicate the telemetry data. This includes, but is not limited to, the changing solar flux, the electrical power output, and the beta prime angle.

## **PART 2: *SENSITIVITY ANALYSIS***

Part 1 outlined the overall thermal system of the satellites and attempted to characterize the thermal variability. Although a rough idea was given of how each of these variables has an effect on the temperatures, they will each now be explored more comprehensively using the Finite Element Method of modeling, as well as a simple generalized energy balance. The first method provides greater details on the temperature variability among the many spacecraft components, whereas the second provides a simplified lumped model for an overall temperature estimation. To reiterate, temperature can change as a result of the various heat sources found internally or externally. The behavior of these sources, as well as the isolated effects they may have on the temperatures, must now be catalogued and considered individually. The remaining three chapters give account of the use of COMSOL Multiphysics and its Finite Element model, as well as a numerical solution to the fundamental heat balance equation, to attempt to link the heat sources to the previously explored temperature fluctuations. Then, the degree of impact for each source can be roughly estimated.



## Chapter 4: The Numerical Model Inputs

Starting with the Finite Element Model produced in COMSOL Multiphysics, this model is derived from several equations to account for heat transfer by way of radiation and conduction. To be thorough, each of these inputs were explored individually and varied to see what sort of effect they might have on the resulting temperature plots. Because this is not a steady-state system, a minimum of a four-day solution to the model was required to allow a temperature equilibrium to be reached to mimic the actual satellite data. A separate analysis of the average satellite temperature was done in MATLAB using conservation of energy principles of the satellite as a whole. The advantage of this second method is that the temperature oscillation rate can much more quickly be extracted and analyzed. The resulting temperature found using these two methods were then compared to thermistor readings directly given by the spacecrafts.

The governing differential equation that serves as the basis for the finite element derivation is the three-dimensional heat equation, shown as Equation 4:

$$\rho c_p \frac{\partial T}{\partial t} + \rho c_p \mathbf{u} \cdot \nabla T = \nabla \cdot (k \nabla T) + \bar{Q} \quad (4)$$

COMSOL automatically discretizes this equation and generates a user-guided model mesh [14]. The initial temperature was set at 293.15 K, and the material-specific properties for each component or surface in the satellite were specified prior to computing the solution.

### SOLAR RADIATION

Transient heat input by way of solar radiation has only three dependencies: The solar constant, the amount of time the satellite spends in the shadow of the earth, and the view factor between each of the individual satellite surfaces and the sun. The beta prime angle has a direct effect on the earth shadow time and the view factor of the satellite

surfaces, so although it will not be directly specified in the model, the resulting effects the beta prime angle has on the spacecraft are taken into account. Therefore, it is not needed to specify the beta prime angle in the model except for the initial calculation of earth shadow time and surface view factors. Taking these three terms into account, COMSOL uses Equation 5 to calculate the solar irradiation  $G_{ext}$  [14]:

$$G_{ext} = F_{ext}(\mathbf{i}_s) \cdot q_{0,s} \quad (5)$$

The view factor  $F_{ext}$  is dependent on the directional vector  $\mathbf{i}_s$ . This is a time-dependent unit vector that is defined by the user as its three separate spatial components. These spatial components were calculated using satellite proximity information and knowledge of sun locations [12]. The source heat flux  $q_{0,s}$  is expanded as Equation 6.

$$q_{0,s} = \eta q_{sol} \quad (6)$$

Its first dependency is fractional coefficient  $\eta$  that varies between 0 for when the satellite is in the earth's shadow, and 1 for when the satellite is in full sunlight. The model, however, estimates  $\eta$  to be  $\frac{1}{2}$  when the satellites are found in the half-shadow zone of Penumbra. Since the amount of time the satellites spend in Penumbra is so small, this approximation is adequate. The value of  $\eta$  at any given time is calculated using simple trigonometric relationships found among the sun, earth, and the altitude of the satellite. It is then inputted directly into the model as a time series variable. This can be visualized in Figure 17.

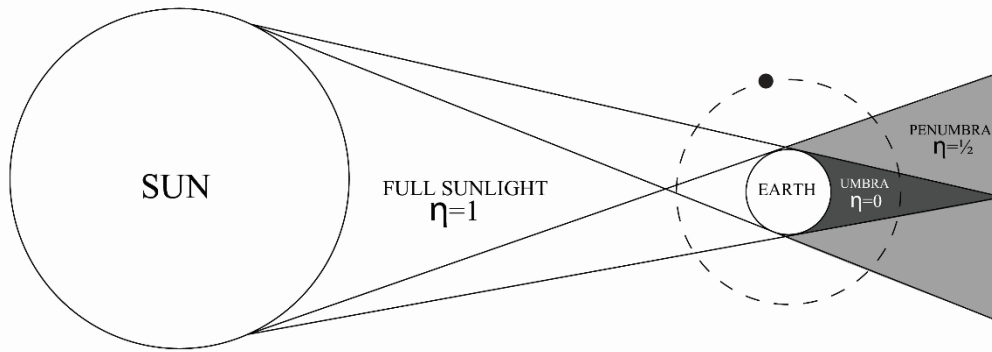


Figure 17: Region of Umbra and Penumbra

The second term in Equation 6, the actual solar flux constant denoted  $q_{sol}$ , is shown in greater detail in the following paragraph. Because the beta prime angle is never explicitly used in the model, variables like  $i_s$  and  $\eta$  were used instead to account for all of the resulting effects. Since the focus of this step in the program is simply to calculate the incoming solar power, the material-specific value of solar absorptivity is included in the overall calculation later.

Although radiation is typically a function of distance, this is not the case in Equation 5. This is because it is convenient to define radiation that comes from the sun to be at an infinite distance. Using commonly accepted values for the solar flux constant (and later for earth infrared radiation and albedo), this distance is already taken into account. The distance from the satellite to the sun does change somewhat for two reasons: it can change with the orbit of the satellite around the earth, and with the annual orbit of the earth around the sun. The former is negligible, however, since the total diameter of this orbit is approximately 7000 km. This amounts to a change of distance from the sun of only 0.04% of the total expanse. However, as mentioned previously, the radius of the earth orbit does

vary somewhat throughout the year, and this does have an effect on the solar flux constant.

Figure 18 is a plot showing this variability [11]:

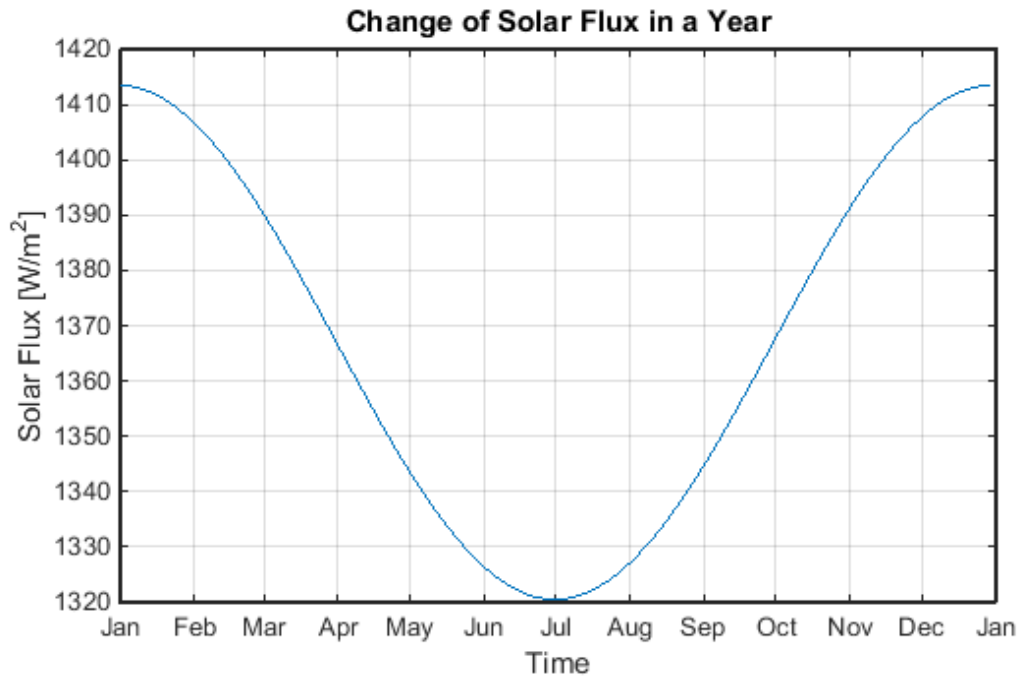


Figure 18: Change of Solar Irradiance

To reduce computation time, the COMSOL model simulates temperatures for only four days at a time. This provides enough time for the simulation to start at an initial temperature of 293 K, and come to a point of equilibrium in the fluctuations. In a four-day time span, the greatest change in the solar flux variable occurs in late March and late September, but the amount is only about  $3 \text{ W/m}^2$ . It was found from multiple computations that the model needed a difference of approximately  $50 \text{ W/m}^2$  to see any effects in the temperatures. As a result, the most common practice was to compute an average solar flux for the time span of interest, and use that for the model input. This then allowed for the variation in the orbit radius of the earth to be taken into account.

## ALBEDO FACTOR

The earth shadow time series given by  $\eta$  has a second use in that the timing of the reflected sunlight almost perfectly matches that of the direct sunlight. Thus, the reflected sunlight by way of the albedo factor is defined in the model in a similar fashion as the direct solar flux, shown in Equation 7:

$$q_{ref} = q_{sol} a_f \eta \quad (7)$$

where the albedo factor  $a_f$  is held at a constant value of 0.3 for the model, which is an average estimated from many different types of surfaces, and over the surface of the earth [2, 4, 6, 9]. This is not, however, a perfect representation of what the satellites truly experience. As stated before, what lies in view of the lower satellite surface is constantly changing over the course of its orbit, especially with changing atmospheric water density and weather patterns. This is not completely random, however, as the poles have a much higher concentration of snow cover, while the equator is more tropical with dense forests [4, 9]. What also changes very little is the orientation of the satellites. Therefore, only three surfaces are exposed, and are always exposed, to this reflected sunlight, and the most uncertainty comes from cloud cover.

## EARTH INFRARED RADIATION

The third heat input to the model represents the heat originating from the earth itself. Since this variable is not dependent on the earth shadow data, nor does the view factor between the satellites and the earth change significantly, this calculation can be simplified. Due to the orientation of the satellites, the only three surfaces that come into contact with this radiation are the bottom and sides orthogonal to the spacecraft x-axis, which is defined as shown earlier in Figure 3 from Chapter 2. Additionally, the latter is

almost perpendicular to the surface of the earth, so a minimal amount of this radiation reaches these two sides. Nevertheless, they are still taken into account.

Infrared radiation from the earth does vary somewhat, but is typically considered constant in satellite thermal balance problems. The model used a constant value of  $234 \text{ W/m}^2$  for this input, but in actuality, the region of the earth around the equator emits more infrared radiation, whereas the region near the poles emit less [2]. It may be prudent in future iterations of the model to account for this, though the change in incoming infrared radiation is small enough compared to the larger solar input to diminish the effect it has on the temperature variability.

#### **RESISTANCE HEATERS AND ELECTRIC CURRENT**

The final inputs to the finite element model and the energy balance analysis include all the heat sources generated by an electric current. Individual heaters were treated as boundary heat sources in the model, and all other components were treated as internal heat sources. The thermally lumped model, however, simply used one total heat generation term to represent the collective electrical components. As stated before, power output was reduced from the heaters when the satellites entered thermal survival mode in 2008, as the thermal tolerances were generally well below what temperature minimums were ever actually being reached. Because of this, power data was used before and after this particular year to gain a more thorough understanding. It must now be noted that even when the heaters were all turned off for an extended period of time after thermal survival mode was in effect, the temperatures extracted from the satellites continued to have a secondary frequency of two cycles per day.

The thermal model does not take small features like wiring, fasteners, harnesses, or small protrusions into account, because of model simplification, incomplete information

and for computational convenience [7]. Because the Finite Element model is missing these small parts, however, it is possible that there is a large sum of thermal mass that is not accounted for. Nevertheless, an assumption was made that the lack of implementation of these small parts do not significantly impact how heat flows through the satellite, and insight was gained from the model in regards to the effects from the major heat sources such as the sunlight and earth infrared. Additionally, it was possible to include the effects of these small parts in the energy balance equation, derived in the next chapter. The reason for this is that the thermal mass is one estimated sum to compute one estimated average temperature for the whole satellite.

## Chapter 5: Results from Numerical Analyses

As previously mentioned, two types of methods were performed using the model inputs listed in the previous chapter: A numerical solution to an overall energy balance of the spacecraft, and a Finite Element Analysis. The value of temperature extracted from the first method was a generalized average using a lumped approximation of the whole system. This provided a rudimentary estimation of what sort of temperature variability was to be expected, given the heat inputs. If the results were incomparable to thermistor readings, it was then known that a thermal input was missing or incorrect. The next section elaborates on this and the derivation of the overall ordinary differential equation, connecting the rate of temperature change with the heat inputs. The Finite Element method provided the means to examine the temperature variability and heat flow through individual components within the spacecraft. The remainder of the chapter will compare the actual thermistor readings to the temperatures extracted from the energy balance estimation as well as the approximations calculated using the Finite Element model.

### ENERGY BALANCE FOR TEMPERATURE ESTIMATION

An equation will now be derived for the purpose of an initial assessment of what temperatures are to be expected in this overall system, since each of the heat inputs have now been categorized. In summary, the three external sources of heat come from direct sunlight  $q_{sol}$ , reflected sunlight  $q_{ref}$ , and infrared radiation from the earth  $q_e$ . Heat is generated in the satellite through electrical loads, and is stored via the satellite's thermal mass. Heat is then emitted primarily by the radiator. As stated before, the system cannot be treated as steady-state, because the amount of energy in the system changes over time. Mathematically, the previous statements can be expressed in the following overall energy balance equation [6]:



$$\dot{Q}_{in} - \dot{Q}_{out} + \dot{Q}_{gen} = \frac{dQ}{dt} \quad (8)$$

Each exterior side of a satellite has a physical property, given through an analysis done by the original thermal engineers, like emissivity  $\varepsilon$  and absorptivity  $\alpha$ . Additionally, each side also has geometric properties like surface area  $A$  and orientation from a heat source  $\theta$  (from the sun) and  $\varphi$  (from the earth), as well as separate temperatures. However, for the purposes of simplification, one average temperature will be used [5]. The first two terms from Equation 8 can now be expanded as such:

$$\begin{aligned} \dot{Q}_{in} &= q_{sol}\eta(\gamma_{sol} + a_f\gamma_e) + q_e\gamma_e \\ \dot{Q}_{out} &= \sum_{j=1}^6 \varepsilon_j \sigma A_j T_j^4 \cong T^4 \sigma \sum_{j=1}^6 \varepsilon_j A_j \end{aligned}$$

Where  $\sigma$  is Stefan-Boltzmann's constant, and  $\gamma_{sol}$  and  $\gamma_e$  are in units of area and take into account surface area, directional cosines, and absorptivity, as shown below:

$$\gamma_{sol} = \alpha_1 A_1 \cos \theta_1 + \alpha_2 A_2 \cos \theta_2 + \alpha_3 A_3 \cos \theta_3 + \alpha_4 A_4 \cos \theta_4 + \alpha_6 A_6 \cos \theta_6$$

$$\gamma_e = \alpha_1 A_1 \cos \varphi_1 + \alpha_2 A_2 \cos \varphi_2 + \alpha_5 A_5 \cos \varphi_5$$

The moving parts within the satellite use a minimal amount of energy, and they only move once every few years, so it can be assumed that all electric power  $P_e$  is converted to heat generated  $\dot{Q}_{gen}$ .

$$\dot{Q}_{gen} = P_e = I v$$

The final term in the energy balance equation concerns itself with the thermal mass of the whole satellite. This is, in other words, the energy stored since the heat is not immediately re-radiated out to space when it enters the system.

$$\frac{dQ}{dt} = mc_p \frac{\partial T}{\partial t}$$

Substituting the above terms, and solving the resulting equation for the time derivative of temperature yields the following non-linear, non-homogeneous, first order governing differential equation for the average temperature fluctuation in the satellite, written as Equation 9.

$$\frac{\partial T}{\partial t} = \frac{q_{sol}\eta(\gamma_{sol}+a_f\gamma_e)+q_e\gamma_e+Iv}{mc_p} - \left( \frac{\sigma \sum_{j=1}^6 \epsilon_j A_j}{mc_p} \right) T^4 \quad (9)$$

The combination of the fourth power in the temperature term in addition to a forcing function being present makes this equation challenging to solve analytically. However, some preliminary information can be gleaned by considering the impact of varying the individual pieces of this expression. For instance, it is known that the forcing function is periodic, and so the temperature change must also be periodic with the same frequencies. However, the dominant frequency is undoubtedly sixteen cycles per day, since the frequency of two cycles per day is only found in the electrical power term. Even within the electrical power data, the frequency of two cycles per day is relatively very small. Thus this lower frequency may be diminished depending on when the data is taken (i.e. after survival mode is initiated). Increasing the average of the forcing function will also increase the temperature rate. Increasing the thermal mass of the system will lower both parts of the right-hand side of the equation. This will result in a lower rate of temperature change, which would mean a smaller amplitude in temperature variability. Now setting aside the thermal mass, the order of the first term is approximately  $10^3$ , whereas the order of the second is  $10^2$ . Consequently, the magnitude of the temperature has less of an impact on the rate of temperature change than does the forcing function, though not significantly less.

To find the equilibrium temperature, the time derivative is set to zero, and the equation is solved for temperature  $T_{eq}$ , shown as Equation 10. The time average of the forcing function  $F_{avg}$  is sufficient to approximate this.

$$F_{avg} = \text{mean}(q_{sol}\eta(\gamma_{sol} + a_f\gamma_e) + q_e\gamma_e + Iv)$$

$$T_{eq} = \left( \frac{F_{avg}}{\sigma \sum_{j=1}^6 \varepsilon_j A_j} \right)^{\frac{1}{4}} \quad (10)$$

Due to the difficulty of analytically solving Equation 9, a numerical method was used. Using the MATLAB numerical differential equation solver `ode45` and the estimated equilibrium temperature as the initial temperature, Equation 9 can be quickly and efficiently computed [13]. The following plot, shown as Figure 19, compares a mass-weighted average temperature telemetry data to the calculated temperature using Equation 9.

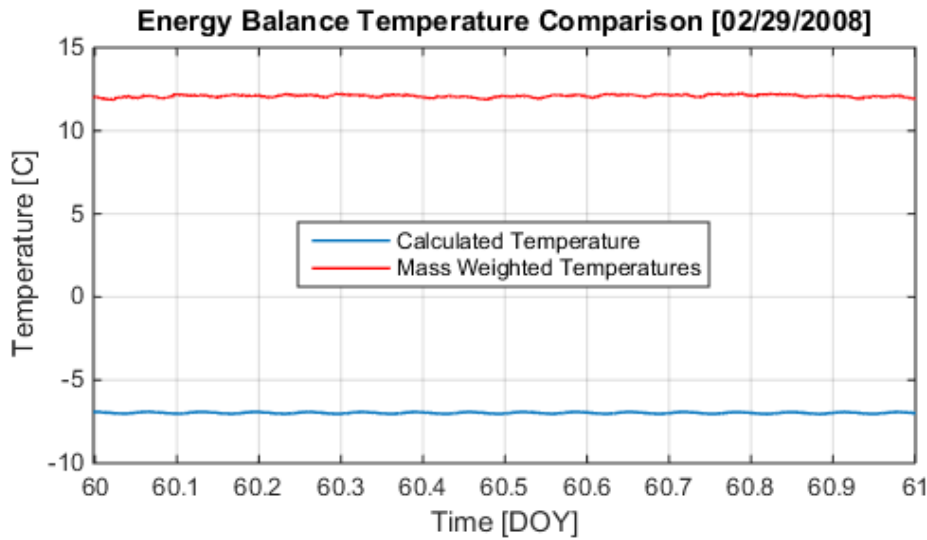


Figure 19: Temperature of Energy Balance vs. Telemetry

Aside from the magnitude difference, a key similarity in the two temperature curves is the amplitude and frequency. Frequency similarity is to be expected since the forcing function, also taken from satellite telemetry, shares this trait. It was previously mentioned that the thermal mass controlled the amplitude, so given the values of the individual thermal masses of the components, this total thermal mass was estimated. The final step is to see if this equation produces a twice per day frequency, as seen in the telemetry temperatures. The following FFT plot, Figure 20, affirms this pattern, though the estimated temperature does have a very small amplitude at two cycles per day:

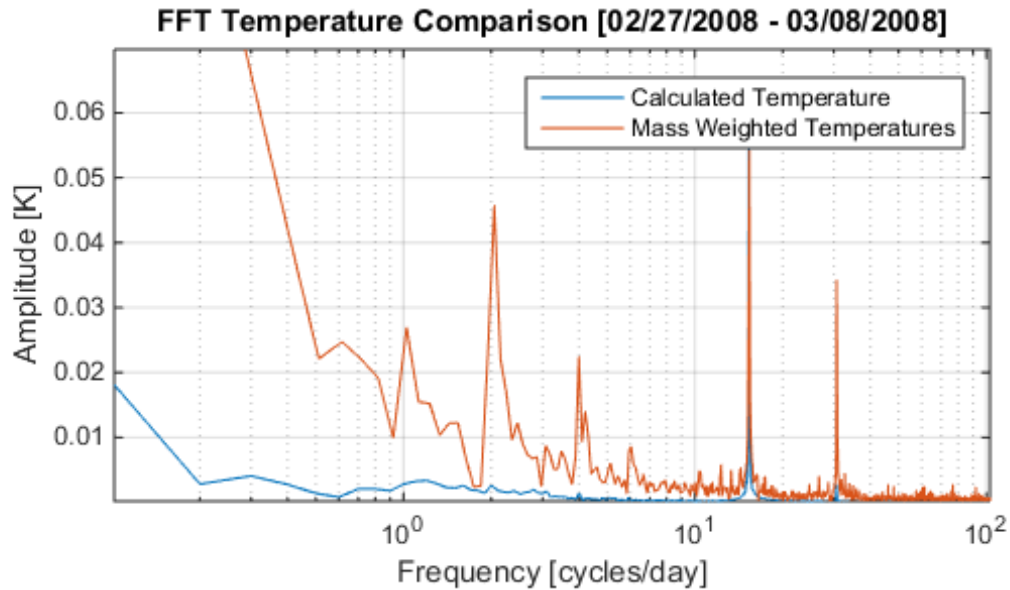


Figure 20: FFT of Energy Balance vs. Telemetry

Not every electrical component within the satellite consistently has a twice per day fluctuation of power. Additionally, since the only term in the energy balance derivation of temperature that has this frequency is the electrical power, the amplitude is minimal. Factors like the location of the thermistors and individual thermal masses may influence why this frequency is so prominent in the telemetry temperature. To reiterate, this

calculated temperature is an average over the entire control volume of the satellite. A future iteration of the heat balance derivation may benefit from having two control volumes: one exclusively around the solar panels of the satellite to solve for an exterior temperature, and a second around the satellite center for finding a separate interior temperature.

## MODEL OUTPUTS

Several temperatures were extracted from the COMSOL model at key locations similar to where the thermistors are located on the actual satellites. The model was tested with three separate cases. The first case excluded all thermal inputs except those that are natural like solar power and earth infrared. Resistance heater output, and later the remaining electrical components, were added. Starting with the first case, Figure 21 compares the telemetry temperatures of the OBDH to the simulation temperatures.

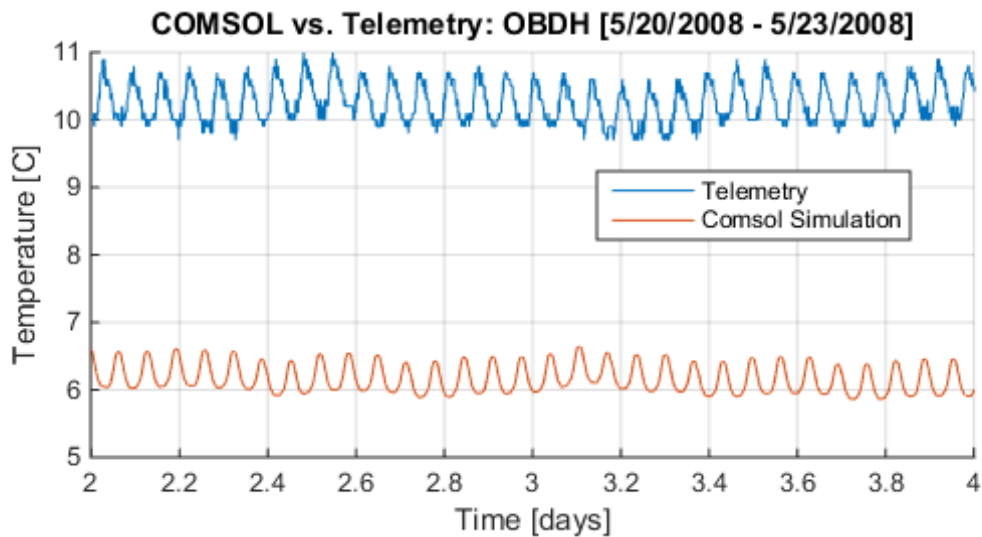


Figure 21: OBDH Telemetry vs. Simulation Temperature: Natural Heat Only

The amplitude of the orbital frequency matches throughout the model, but the overall magnitude does not. This is an expected result as there are no electrical components

enabled. There is also no twice-per-day frequency, since the external heat sources also do not have this frequency. The next step is to add all the heaters as boundary heat sources. From the initial temperature analysis, it was mentioned that the heaters fluctuate two times in a day, so it is to be expected that this frequency will appear in the resulting thermal model temperatures. The following plot, Figure 22, is the OBDH temperatures with the heaters added.

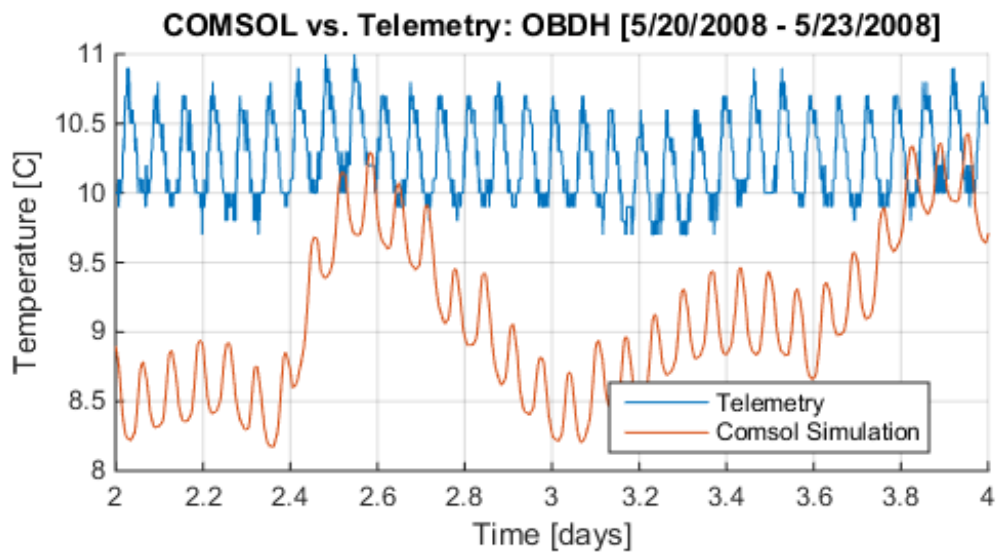


Figure 22: OBDH Telemetry vs. Simulation Temperature: Natural Heat and Heaters

The magnitude of the simulation temperatures are now closer to that of the telemetry temperatures, and the primary orbital frequency is retained. However, the response is much less regular and the frequency of two cycles per day does not appear in these results. Finally, the following plot, Figure 23, has all heat inputs.

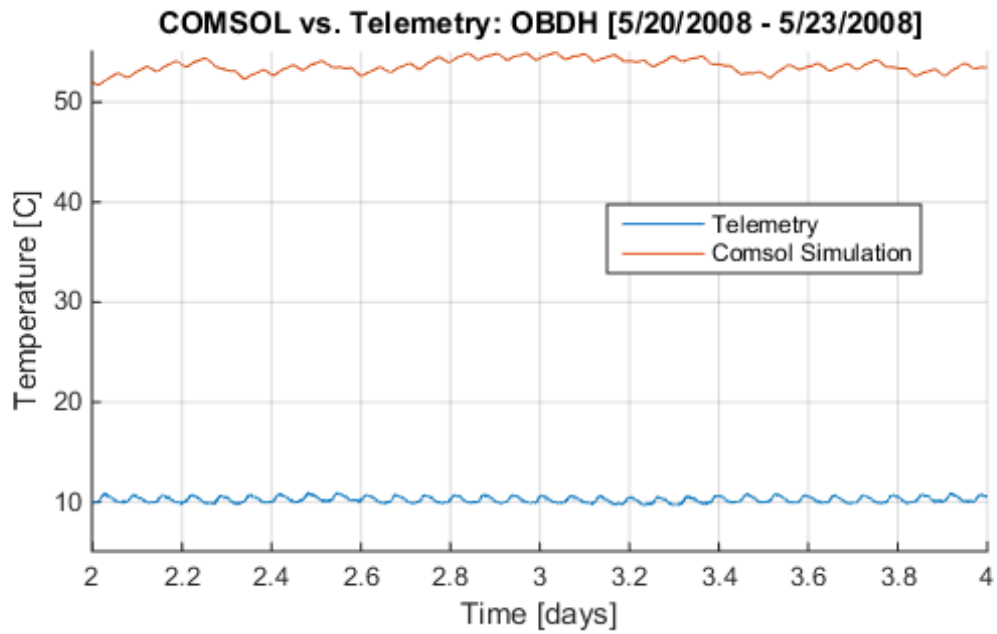


Figure 23: OBDH Telemetry vs. Simulation Temperature: All Heat Inputs

The amplitude of the orbital frequency is retained. However, the result of including all heat inputs is that there is a much higher temperature magnitude, as well as an irregular secondary frequency.

## **Chapter 6: Conclusions and Suggestions**

The overall goal of the thermal analysis of the GRACE Twin Satellites was to gain a more thorough understanding of temperature fluctuations throughout each spacecraft, so that a reasonable estimation for thermal expansion may be derived by future researchers. There are a few steps to be taken prior to exploring this relationship between the temperature variability and the thermal expansion, but there are some new insights into the satellite system from this project. These insights started with an initial overview of the satellites' temperatures taken from several locations, and over the duration of many different time intervals. When analyzing these temperatures, it was found that they fluctuate at the same rate as the satellite orbit at 16 cycles per day, but an additional frequency of two cycles per day was revealed. For future researchers to completely understand the spacecraft thermal environment, it was necessary to trace the source of this oscillation rate.

By individually investigating each of the thermal inputs to the satellites, it was evident what factor has the greatest influence on the resulting overall temperatures: direct sunlight. Due to the surface area of each satellite, they were able to absorb as much as 5500 watts from sunlight alone when the beta prime angle was low, and as much as 2700 watts when the beta prime angle was high, which is reflected in the temperature magnitude at these respective events. A single frequency of 16 cycles per day was found coming from the direct sunlight, which matched the primary frequency of the satellite temperature variations, aside from the long-term effects of the earth orbit eccentricity. This pattern is shown in Figure 24, whose data is taken from May of 2008:



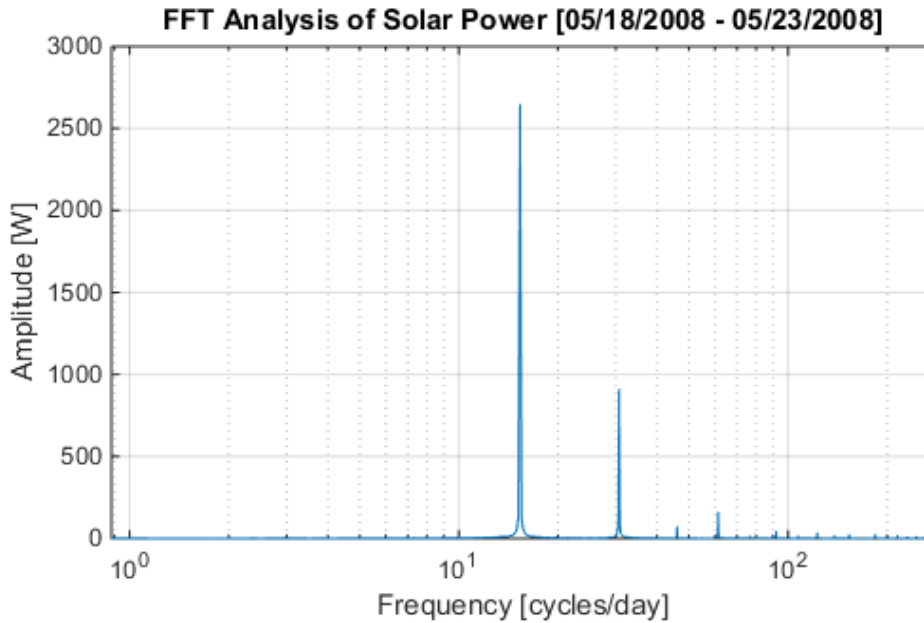


Figure 24: FFT Plot of Total Incoming Solar Power

The temperatures fluctuated at this rate even when the satellites spent extended periods of time in full sunlight- when the beta prime angle was high. The reason for this is that although the satellites go for long periods of time without entering the shadow of the earth while the beta prime angle is high, the view factor is continuously changing with the orbital motion. The maximized beta prime angle, therefore, will not eliminate the orbital frequency effects altogether, but will certainly change the amplitude, and the resulting temperatures.

The earth infrared radiation was set to a constant value of  $234 \text{ W/m}^2$  for the duration of this project. It would therefore not contribute to the oscillation rate found in the resulting temperature variability of the energy balance solution or the Finite Element simulation. The second earth output, the albedo, was dependent upon the timing factor  $\eta$  as well as the magnitude of the incoming solar flux. The albedo yield consequently has the satellite orbital frequency of 16 cycles per day, but not the secondary twice per day frequency. In

reality, these two terms vary with the orbital motion of the satellites, and implementing this in future calculations would be a viable next step.

The final heat input, which was generated via waste heat from the electrical power, contributed as much as 2200 watts while the beta prime angle was low, and 550 watts when the beta prime angle was high. This places electrical power as the second greatest heat source. Since the electrical power is contingent upon the availability of sunlight, this also had a frequency of 16 cycles per day. Electrical power was the only thermal energy source studied that had the additional twice per day variation, though it was sometimes diminished by the larger frequencies. An extensive examination of each of the individual electrical elements then led to an overall perspective of which components always have this frequency, and which may be otherwise less regular.

As mentioned before, the heaters followed this low fluctuation rate most of the time, but were much less active after the satellites entered thermal survival mode, and can thus be eliminated as a possible cause of the temperatures having this low frequency. Other components were also studied, but the power output of most did not persistently oscillate at this rate. However, the transmitter, the component tasked with relaying telemetry data back to researchers, was found to always have this secondary fluctuation rate even after the thermal survival mode begun, as shown in Figure 25. The transmitter consumes power at this rate because it is programmed to transfer the information twice every day.

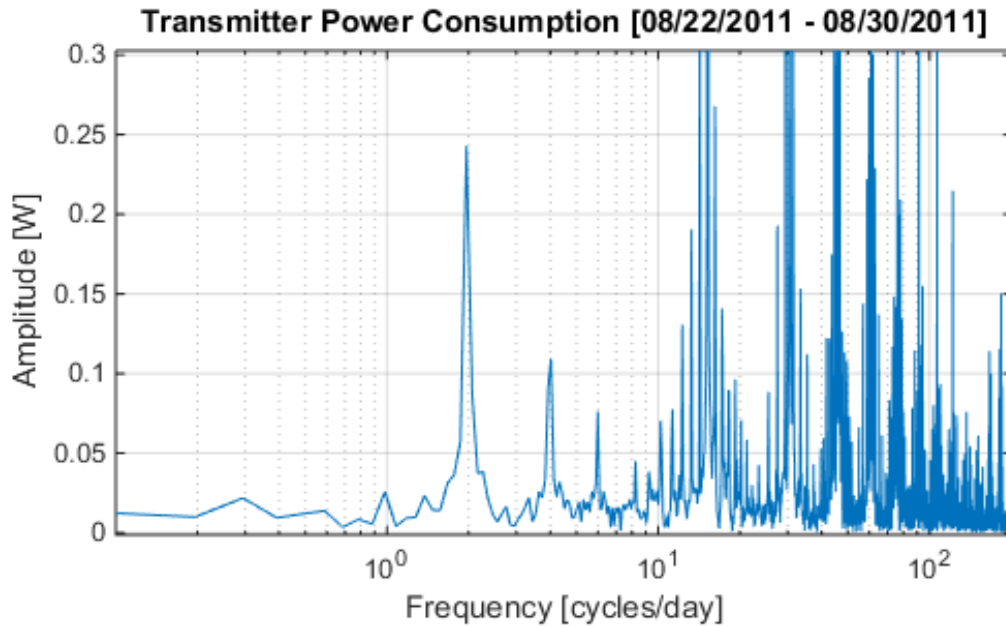


Figure 25: FFT Plot of Transmitter Power

The transmitter activates twice every day regardless of the surrounding environment. This then draws power from the satellite batteries twice every day, which will then cause the remaining electrical components to lose power. Consequently, the remaining electrical components will share this twice per day frequency. As a result, the temperature of each satellite will oscillate from the periodic change in the electrical power.

Two methods were used to verify this hypothesis: A numerical solution to the fundamental conservation of energy principle, and the use of a Finite Element Analysis. The Finite Element model produced in COMSOL gave some insight to how temperature varies in each of the individual components, but a completely accurate model was never achieved, and two cycles per day were never observed in the resulting temperature plots. The generalized solution to the energy balance equation thus proved more useful for this verification, using a lumped thermal model approximation. However, it is possible that a more accurate expression may be derived by splitting the satellite control volume into an

external balance and an internal balance. This will then take conduction among the internal components into account as well as any insulation separating the outside panels from the spacecraft interior. However, this modified energy balance may also introduce more error into the approximation. The reason for this is that not only will thermal mass need to be estimated, but other properties such as conductivity, emissivity, and absorptivity will need to be as well. Even so, it was unnecessary to pursue a modification of the energy balance derivation, as the goal of this particular research project was to locate the source of the two cycle per day frequency, which was achieved.

## Glossary

$a_f$  – Albedo factor

$A_j$  – Area of spacecraft side  $j$ , where  $j = 1, 2, \dots, 6$  [meter<sup>2</sup>]

$c_p$  – Specific heat capacity estimation of spacecraft [Joule/kilogram-Kelvin]

$F_{avg}$  – Time average of forcing function of fundamental energy balance differential equation [Watt]

$F_{ext}$  – View factor from the spacecraft to the sun

$G_{ext}$  – Solar irradiation variable used by COMSOL [Watt/meter<sup>2</sup>]

$\mathbf{i}_s$  – Unit vector location of sun with respect to the satellite

$I$  – Electrical current [Ampere]

$k$  – Thermal conductivity [Watt/meter-Kelvin]

$m$  – Mass estimation of spacecraft [kilogram]

$P_e$  – Total electrical power consumption [Watt]

$P_{heater}$  – Heater power output [Watt]

$P_i$  – Component power consumption where  $i$  is component number [Watt]

$Q$  – Heat transferred [Joule]

$\bar{Q}$  – Overall forcing function of heat transfer per unit volume used by COMSOL [Watt/meter<sup>3</sup>]

$q_{0,s}$  – Direct solar flux that impacts the spacecraft [Watt/meter<sup>2</sup>]

$q_{actual}$  – Solar radiation that satellite receives [Watt/meter<sup>2</sup>]

$q_e$  – Earth infrared radiation flux [Watt/meter<sup>2</sup>]

$\dot{Q}_{gen}$  – Waste heat generated within spacecraft [Watt]

$\dot{Q}_{in}$  – External heat power absorbed by spacecraft [Watt]

$\dot{Q}_{out}$  – Heat power emitted by spacecraft to the environment [Watt]

$q_{ref}$  – Reflected solar flux that impacts the spacecraft [Watt/meter<sup>2</sup>]  
 $q_{sol}$  – Solar flux constant [Watt/meter<sup>2</sup>]  
 $R$  – Resistance [Ohm]  
 $T$  – Temperature [Kelvin]  
 $t$  – Time [second]  
 $T_{eq}$  – Estimated equilibrium temperature [Kelvin]  
 $\mathbf{u}$  – Velocity vector [meter/second]  
 $v$  – Battery voltage [Volt]  
 $\alpha_j$  – Absorptivity of surface  $j$ , where  $j = 1, 2, \dots, 6$   
 $\gamma_e$  – Surface factor with respect to the earth [meter<sup>2</sup>]  
 $\gamma_{sol}$  – Surface factor with respect to the sun [meter<sup>2</sup>]  
 $\delta$  – Boolean variable representing the on/off state of heater power output  
 $\eta$  – Earth eclipsing coefficient  
 $\theta_j$  – Angle between incoming solar rays and surface  $j$  normal, where  $j = 1, 2, \dots, 6$   
 $\varphi_j$  – Angle between incoming earth radiation and surface  $j$  normal, where  $j = 1, 2, \dots, 6$   
 $\varepsilon_j$  – Emissivity of spacecraft side  $j$ , where  $j = 1, 2, \dots, 6$   
 $\rho$  – Material density [kilogram/meter<sup>3</sup>]  
 $\sigma$  – Stefan-Boltzmann's constant [Watt/meter<sup>2</sup>-Kelvin<sup>4</sup>]

## References

- Vieira, L. E., Solanki, S. K., Krivova, N. A., & Usoskin, I. (2011). Evolution of the solar irradiance during the Holocene. *A&A*, 531. Retrieved January 25, 2016, from <https://www-engineeringvillage-com.ezproxy.lib.utexas.edu/search/quick.url>.
- Earth's Thermal Environment. (2008). Retrieved March 20, 2016, from <http://www.tak2000.com/data/planets/earth.htm>
- Eccentricity. (n.d.). Retrieved March 20, 2016, from [http://ffden-2.phys.uaf.edu/212\\_fall2003.web.dir/Beth\\_Caissie/eccentricity.htm](http://ffden-2.phys.uaf.edu/212_fall2003.web.dir/Beth_Caissie/eccentricity.htm)
- Bortman, M., & Abbey, E. P. (2003). A. In *Environmental Encyclopedia* (3rd ed., Vol. 1, A-M, p. I: 38). Farmington Hills, MI: The Gale Group.
- Pryzby, M. (2011). Spacecraft Subsystems V- Structures and Thermal. In *Space Mission Engineering: The New SMAD* (pp. 685-700). Hawthorn, CA: Microcosm Press.
- Panetti, A., & McMordie, R. K. (1999). Thermal. In *Spacecraft Mission Analysis and Design* (3rd ed., pp. 428-458). Hawthorn, CA: Microcosm Press.
- Jones, F. (2013). *Report.docx*. Unpublished manuscript, University of Texas, USA.
- Palle, E. (2004). Changes in the Earth's reflectance over the past two decades. Retrieved July 18, 2016, from [http://lasp.colorado.edu/sdo/meetings/session\\_1\\_2\\_3/presentations/session3/3\\_06\\_Palle.pdf](http://lasp.colorado.edu/sdo/meetings/session_1_2_3/presentations/session3/3_06_Palle.pdf)
- Coakley, J. A. (2003). REFLECTANCE AND ALBEDO, SURFACE. Retrieved July 18, 2016, from [http://curry.eas.gatech.edu/Courses/6140/ency/Chapter9/Ency\\_Atmos/Reflectance\\_Albedo\\_Surface.pdf](http://curry.eas.gatech.edu/Courses/6140/ency/Chapter9/Ency_Atmos/Reflectance_Albedo_Surface.pdf)
- Watkins, T. (n.d.). The Net Effect of Cloudiness on Surface Temperatures. Retrieved July 18, 2016, from <http://www.sjsu.edu/faculty/watkins/cloudiness.htm>

Solar Energy Reaching the Earth's Surface. (n.d.). Retrieved March 23, 2016, from <http://www.itacanet.org/the-sun-as-a-source-of-energy/part-2-solar-energy-reaching-the-earths-surface/>

Ling, F., & Ries, J. (2015). *shadow.m*. MATLAB™ code. University of Texas, USA.

MATLAB 2014b, The MathWorks, Inc., Natick, Massachusetts, United States.

COMSOL Multiphysics 4.4, COMSOL, Inc., Palo Alto, California, United States.

Bettadpur, S. (2016, August 1). Personal communication.